EUROPEAN ORGANIZATION FOR NUCLEAR RESEARCH (CERN)

CERN-EP-2019-171
2019/08/23

CMS-SUS-18-007

Search for supersymmetry using Higgs boson to diphoton decays at $\sqrt{s} = 13\,\text{TeV}$

The CMS Collaboration*

Abstract

A search for supersymmetry (SUSY) is presented where at least one Higgs boson is produced and decays to two photons in the decay chains of pair-produced SUSY particles. Two complementary analysis strategies are pursued: one focused on strong SUSY production and the other focused on electroweak SUSY production. The presence of charged leptons, additional Higgs boson candidates, and various kinematic variables are used to categorize events into search regions that are sensitive to different SUSY scenarios. The results are based on data from proton-proton collisions at the Large Hadron Collider at a center-of-mass energy of 13 TeV collected by the CMS experiment, corresponding to an integrated luminosity of 77.5 fb^{-1}. No statistically significant excess of events is observed relative to the standard model expectations. We exclude bottom squark pair production for bottom squark masses below 530 GeV and a lightest SUSY particle mass of 1 GeV; wino-like chargino-neutralino production for chargino and neutralino masses below 235 GeV with a gravitino mass of 1 GeV; and higgsino-like chargino-neutralino production in the case where the neutralino decays exclusively to a Higgs boson and a gravitino for neutralino masses below 290 GeV.

Submitted to the Journal of High Energy Physics

*See Appendix B for the list of collaboration members

1 Introduction

The Higgs boson (H) provides an intriguing opportunity to explore physics beyond the standard model (SM) of particle physics. Many scenarios of physics beyond the SM postulate the existence of cascade decays of heavy states involving Higgs bosons [1, 2]. In minimal supersymmetry (SUSY) [3], a Higgs boson may appear in processes involving the bottom squark ($\widetilde{\mathrm{b}}$), the SUSY partner of the bottom quark. Bottom squarks are produced via strong interactions and then may decay to a Higgs boson, quarks, and the lightest SUSY particle (LSP). Similarly charginos or neutralinos produced through the electroweak interaction may decay to a Higgs boson and the LSP. Of particular interest are gauge-mediated SUSY breaking (GMSB) scenarios, where the lightest neutralino may decay to a Higgs boson and the gravitino LSP ($\widetilde{\mathrm{G}}$) [4, 5]. The decay signature in this case changes according to whether the chargino and neutralino mixed states are dominated by the wino or higgsino components, the respective SUSY partners of the W and Higgs bosons. Similar searches have been performed by the ATLAS and CMS Collaborations using proton-proton (pp) collisions at the CERN LHC at center-of-mass energies of 8 [6, 7] and 13 TeV [8, 9].

We search for evidence of SUSY that produces an excess of events with one or more Higgs bosons and large missing transverse momentum using pp collision data collected by the CMS experiment at the LHC at a center-of-mass energy of 13 TeV in 2016 and 2017, corresponding to an integrated luminosity of 77.5 fb^{-1}. Kinematic variables that discriminate the SUSY signal from SM backgrounds are used to separate events into several mutually exclusive categories, and the diphoton mass from the $\mathrm{H} \to \gamma\gamma$ decay is used to extract the signal from the background. The dominant backgrounds are SM production of diphoton and photon+jets, which are modeled by functional fits to the diphoton mass distribution.

We have designed a new analysis to extend our sensitivity to both strong and electroweak SUSY production over the previously published result [8]. Two complementary analysis strategies are pursued: one focuses on the electroweak production of charginos and neutralinos by introducing additional event categories containing one or two charged-lepton candidates, thereby enhancing the sensitivity to SUSY signatures involving W and Z bosons, and the other is optimized for strong production by categorizing events in the number of jets and the number of jets identified as originating from the fragmentation of b quarks ("b-tagged"). The use of the two complementary strategies enhances the overall sensitivity of the search, and increases the robustness of the result by exploring alternative phase space regions. Finally, we interpret the results in various simplified model scenarios of SUSY as summarized in Fig. 1, including bottom squark pair production, chargino-neutralino, and neutralino-pair production.

In this paper, we discuss the CMS detector in Section 2, the event simulation in Section 3, the event reconstruction and selection in Section 4, the analysis strategy in Section 5, the background estimation in Section 6, the systematic uncertainties in Section 7, and the results and interpretations in Section 8. A summary is given in Section 9.

2 The CMS detector

The central feature of the CMS detector is a superconducting solenoid of 6 m internal diameter, providing a magnetic field of 3.8 T. Within the solenoid volume are a silicon pixel and strip tracker, a lead tungstate crystal electromagnetic calorimeter (ECAL), and a brass and scintillator hadron calorimeter, each composed of a barrel and two endcap sections. Forward calorimeters extend the pseudorapidity (η) coverage provided by the barrel and endcap detectors. Muons are measured in gas-ionization detectors embedded in the steel flux-return yoke outside the

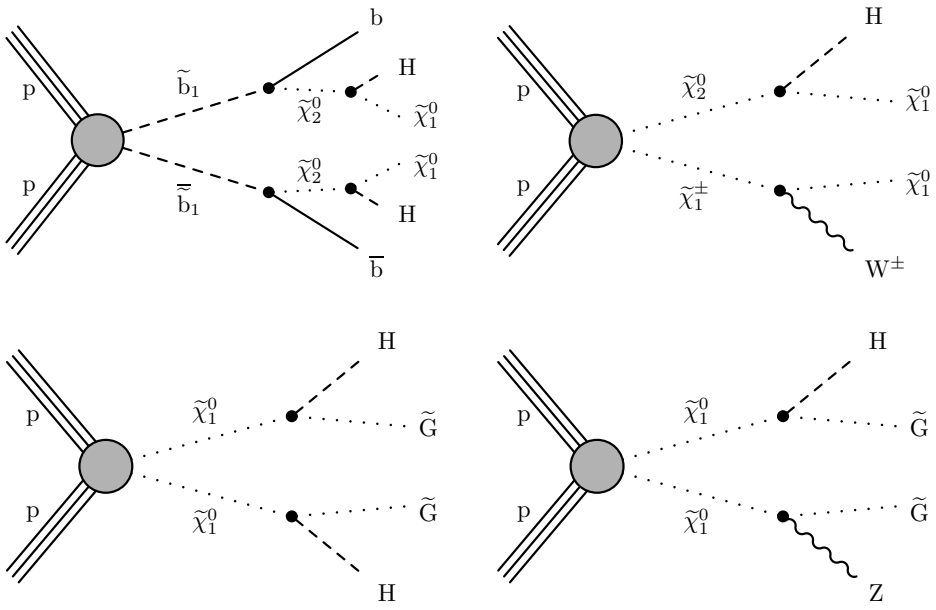

Figure 1: Diagrams displaying the simplified models that are being considered. Upper left: bottom squark pair production; upper right: wino-like chargino-neutralino production; lower: the two relevant decay modes for higgsino-like neutralino pair production in the GMSB scenario.

solenoid. The first level of the CMS trigger system [10], composed of custom hardware processors, uses information from the calorimeters and muon detectors to select the most interesting events in a fixed time interval of less than 4 μs. The high-level trigger processor farm further decreases the event rate from around 100 kHz to less than 1 kHz before data storage. A more detailed description of the CMS detector, together with a definition of the coordinate system used and the relevant kinematic variables, can be found in Ref. [11].

3 Event simulation

Simulated Monte Carlo (MC) event samples are used to model the SM Higgs boson backgrounds and the SUSY signal models. Simulated samples of SM Higgs boson production through gluon fusion, vector boson fusion, associated production with a W or a Z boson, $b\bar{b}H$, and $t\bar{t}H$ are generated using the next-to-leading order (NLO) MADGRAPH5_aMC@NLO v2.2.2 [12] event generator. The Higgs boson mass is assumed to be 125 GeV for the simulated event samples and is within the uncertainty of the currently best measured value [13, 14]. The Higgs boson production cross sections are taken from Ref. [15] and are computed to next-to-next-to-leading order plus next-to-next-to-leading logarithm in the quantum chromodynamics (QCD) coupling constant and to NLO in the electroweak coupling constant. For the gluon fusion production mode, the sample is generated with up to two extra partons from initial-state radiation (ISR) at NLO accuracy and used the FxFx matching scheme described in Ref. [16]. The SUSY signal MC samples are generated using MADGRAPH5_aMC@NLO at leading order accuracy with up to two extra partons in the matrix element calculations, with the MLM matching scheme described in Ref. [17]. For samples simulating the 2016 data set, PYTHIA v8.212 [18] is used to model the fragmentation and parton showering with the CUETP8M1 tune [19], while for samples simulating the 2017 data set, PYTHIA v8.226 is used with the CP5 [20] tune. The NNPDF3.0 [21] and NNPDF3.1 [22] parton distribution function (PDF) sets are used for the 2016 and 2017 simulation samples, respectively.

The SM Higgs boson background samples are simulated using a GEANT4-based model [23] of the CMS detector. To cover the large SUSY signal parameter space in reasonable computation time, the signal model samples are simulated with the CMS fast simulation package [24, 25], which has been validated to produce accurate predictions of object identification efficiencies and momentum resolution. All simulated events include the effects of additional pp interactions in the same or adjacent beam bunch crossings (pileup), and are processed with the same chain of reconstruction programs used for collision data.

To improve the MADGRAPH modeling of ISR in the SUSY signal MC samples, we apply a shape correction as a function of the multiplicity of ISR jets for bottom squark pair production and as a function of the transverse momentum ($p_{\mathrm{T}}^{\mathrm{ISR}}$) of the chargino-neutralino system for chargino-neutralino production, derived from studies of $\mathrm{t\bar{t}}$ and Z +jets events, respectively. The correction factors vary between 0.92 and 0.51 for the ISR jet multiplicity between one and six, and between 1.18 and 0.78 for $p_{\mathrm{T}}^{\mathrm{ISR}}$ between 125 and 600 GeV. The correction has a small effect on the signal yields at the level of about 1%. For the bottom squark pair production signal model, the correction is larger and the full effect of the correction is propagated as a systematic uncertainty. For the chargino-neutralino production one half of effect of the correction is propagated as a systematic uncertainty.

4 Event reconstruction and selection

The search with the 2016 data set uses events selected by the diphoton high-level trigger, which requires two photons with p_{T} above 30 and 18 GeV for the leading and subleading photons, respectively. For the 2017 data set, to cope with the increased instantaneous luminosity, the p_{T} requirement on the subleading photon was increased to 22 GeV in order to reduce the trigger rate.

Events are reconstructed using the CMS particle flow (PF) algorithm [26], which uses the information from the tracker, calorimeter, and muon systems to construct an optimized global description of the event. As the signal is predominantly produced in the central region of the detector, we select events with at least two photons reconstructed in the barrel region ($|\eta| < 1.44$). The photons are required to satisfy the photon identification requirements based on electromagnetic shower shape, hadronic to electromagnetic energy ratio, and isolation around the photon candidate. A photon is considered isolated if the p_{T} sum of the PF candidates from charged and neutral hadrons and photons within a cone of 0.3 in $\Delta\mathrm{R} = \sqrt{(\Delta\eta)^2 + (\Delta\phi)^2}$, where phi is the azimuthal angle in radians, are each below a set threshold. The isolation sums are corrected for the effect of pileup by subtracting the average energy deposited as estimated by the pileup energy density ρ [27]. If the photon is matched to a reconstructed electron that is inconsistent with a conversion candidate, it is discarded. A loose working point is used for the photon identification, which has an efficiency of approximately 90%. The leading (subleading) photon is required to have $p_{\mathrm{T}}/m_{\gamma\gamma} > 0.33$ (0.25), where $m_{\gamma\gamma}$ is the reconstructed diphoton mass. The diphoton mass is required to be larger than 100 GeV. The two photons with the largest p_{T}, selected according to the identification criteria above, are considered to be the decay products of the Higgs boson candidate.

The PF candidates are clustered into jets using the anti-k_{T} algorithm [28, 29] with a distance parameter of 0.4. Jet energy corrections are applied and derived based on a combination of simulation studies, accounting for the nonlinear detector response and the presence of pileup, together with in-situ measurements of the energy balance in dijet and γ+jet events using the methods described in Ref. [30]. Jets originating from a heavy-flavor parton are identified by

the combined secondary vertex (CSVv2) tagger algorithm [31] using a loose working point. The resulting efficiency is about 80%, while the mistag rate for light-quark and gluon jets is approximately 10%. We identify each jet with $p_{\mathrm{T}} > 20\,\mathrm{GeV}$ that satisfies the loose working point as a b-tagged jet. Other jets with $p_{\mathrm{T}} > 30\,\mathrm{GeV}$ and $|\eta| < 2.4$ are considered in this analysis for the purpose of jet counting. Electrons and muons in the region $|\eta| < 2.4$ and with $p_{\mathrm{T}} > 20\,\mathrm{GeV}$ are selected from the PF candidates, and a loose identification working point is used. Jets that overlap with the selected electrons, muons, and photons in a cone of size $\Delta\mathrm{R} = 0.4$ are discarded. Electrons in a cone of size $\Delta\mathrm{R} = 1.0$ and muons in a cone of size $\Delta\mathrm{R} = 0.5$ around the selected photons are discarded. A larger veto cone is used for electrons to suppress photon conversions.

The transverse component of the negative vectorial sum of the momenta of all PF candidates is the missing transverse momentum $\vec{p}_{\mathrm{T}}^{\,\mathrm{miss}}$, and its magnitude is defined as $p_{\mathrm{T}}^{\mathrm{miss}}$. Dedicated filters [32] reject events with possible beam halo contamination or anomalous noise in the calorimeter systems that can give rise to a large $p_{\mathrm{T}}^{\mathrm{miss}}$.

5 Analysis strategy

Two complementary analysis strategies are pursued that employ two alternative event categorization schemes: one focused on electroweak production (EWP analysis) of charginos and neutralinos; and another focused on strong production (SP analysis) of bottom squarks. For both strategies, we define event categories that are sensitive to the p_{T} of the diphoton Higgs boson candidate, and the presence of additional Z, W, or $\mathrm{H} \to \mathrm{b\bar{b}}$ candidates. Within each event category, we define search region bins based on the number of jets and b-tagged jets, and the values of kinematic variables that discriminate between SUSY signal and SM backgrounds events. Finally, to test specific SUSY simplified model hypotheses, we perform a combined simultaneous fit to the diphoton mass distribution in all of the search bins defined for each analysis. The dominant background results from SM production of diphoton or photon+jets, and is collectively referred to as the nonresonant background. This background is modeled with a fit to a family of falling functions independently in each search region bin as described in the next section. The SM Higgs boson background and the SUSY signal model under test exhibit a resonant shape in the diphoton mass and are constrained to the MC simulation predictions within uncertainties. A more detailed discussion of the background fit model and the systematic uncertainties can be found in Sections 6 and 7, respectively.

In the EWP approach, we build upon the strategy employed in a previous publication [8], which categorized events according to the p_{T} of the diphoton Higgs boson candidate, the presence of an additional Higgs boson candidate, the estimated diphoton mass resolution, and the values of the "razor" kinematic variables [33, 34]. In addition, we add event categories with one or two identified leptons, and further optimize the binning in the kinematic variables for the enlarged data set. These enhancements improve the signal sensitivity to electroweak production of charginos and neutralinos. By isolating events with a Z, W, or $\mathrm{H} \to \mathrm{b\bar{b}}$ candidate in addition to the $\mathrm{H} \to \gamma\gamma$ candidate, we improve the sensitivity to the simplified signal models shown in Fig. 1.

The Higgs boson candidate and any additional identified leptons or jets are clustered into two hemispheres (megajets) according to the razor megajet algorithm [34], which minimizes the sum of the squared-invariant-mass values of the two megajets. In order to form two hemispheres, we require that events have at least one identified lepton or jet in addition to the

Higgs boson candidate. The razor variables [33, 34] M_{R} and R^2 are then computed as follows:

$$M_{\mathrm{R}} \equiv \sqrt{(|\vec{p}^{\,\mathrm{j}_1}| + |\vec{p}^{\,\mathrm{j}_2}|)^2 - (p_z^{\,\mathrm{j}_1} + p_z^{\,\mathrm{j}_2})^2}, \tag{1}$$

$$R^2 \equiv \left(\frac{M_{\mathrm{T}}^{\mathrm{R}}}{M_{\mathrm{R}}}\right)^2, \tag{2}$$

where $\vec{p}$ is the momentum of a megajet, p_z is its longitudinal component, and j_1 and j_2 are used to label the two megajets. In the definition of R^2, the variable $M_{\mathrm{T}}^{\mathrm{R}}$ is defined as:

$$M_{\mathrm{T}}^{\mathrm{R}} \equiv \sqrt{\frac{p_{\mathrm{T}}^{\mathrm{miss}}(p_{\mathrm{T}}^{\,\mathrm{j}_1} + p_{\mathrm{T}}^{\,\mathrm{j}_2}) - \vec{p}_{\mathrm{T}}^{\,\mathrm{miss}} \cdot (\vec{p}_{\mathrm{T}}^{\,\mathrm{j}_1} + \vec{p}_{\mathrm{T}}^{\,\mathrm{j}_2})}{2}}. \tag{3}$$

The razor variables M_{R} and R^2 provide discrimination between SUSY signal models and SM background processes, with SUSY signals typically having large values of M_{R} and R^2, while the SM diphoton and photon+jets backgrounds exhibit a falling spectrum in each variable.

The selected events are first categorized according to the number of electrons or muons. Events with two same-flavor opposite-sign leptons are placed in the "Two-Lepton" category if the dilepton mass satisfies the constraint $|m_{\mathrm{Z}} - m_{\ell\ell}| \leq 20\,\mathrm{GeV}$. Among the remaining events, those with at least one muon (electron) are placed in the "Muon" ("Electron") category, with the Muon category taking precedence. Events in the Electron and Muon categories are further subdivided into the "High-p_{T}" and "Low-p_{T}" subcategories depending on whether the p_{T} of the Higgs boson candidate is larger or smaller than 110 GeV. For events which do not have any leptons, we search for pairs of b-tagged jets, whose mass is between 95 and 140 GeV, and place them into the "H$\mathrm{b\bar{b}}$" category. If no such jet-pairs are found, then we search for pairs of b-tagged jets whose mass is between 60 and 95 GeV, and place them into the "Z$\mathrm{b\bar{b}}$" category. Events in the H$\mathrm{b\bar{b}}$ and Z$\mathrm{b\bar{b}}$ categories are also further subdivided into the High-p_{T} and Low-p_{T} subcategories using the same criteria stated above. Among the remaining events, those with the p_{T} of the Higgs boson candidate larger than 110 GeV are placed in the High-p_{T} category. Finally, the remaining events are categorized as "High-Res" or "Low-Res" if the diphoton mass resolution estimate σ_m/m is smaller or larger than 0.85%, respectively, with σ_m defined as:

$$\sigma_m = \frac{1}{2}\sqrt{(\sigma_{E\gamma 1}/E_{\gamma 1})^2 + (\sigma_{E\gamma 2}/E_{\gamma 2})^2}, \tag{4}$$

where $E_{\gamma 1,2}$ is the energy of each photon and $\sigma_{E\gamma 1,2}$ is the estimated energy resolution for each photon. The photon energy resolution is estimated by a multivariate regression estimator based on a boosted decision tree that uses a combination of energy and shower shape measurements from the ECAL.

The leptonic categories select SUSY events containing decays to W or Z bosons; the H$\mathrm{b\bar{b}}$ (Z$\mathrm{b\bar{b}}$) categories select events that contain an additional Higgs (Z) boson, which decays to a pair of b jets; the High-p_{T} category selects SUSY events producing high-p_{T} Higgs bosons; and the separation into the High-Res and Low-Res categories further improves the discrimination between signal and background in the remaining event sample. Finally, to distinguish SUSY signal events from the SM background, each event category is further divided into bins in the M_{R} and R^2 variables, provided there are a sufficient number of data events in the diphoton mass sideband to be able to estimate the background. Finally, these bins define the exclusive search regions. For all categories except the Two-Lepton category, we impose the requirement $M_{\mathrm{R}} > 150\,\mathrm{GeV}$ to suppress the SM backgrounds. For signal models in the uncompressed region of SUSY parameter space, where a large mass splitting between the parent particle and

its decay products results in final state particles with large transverse momentum, the High-p_{T} category provides the best sensitivity. For signal models in the compressed region of parameter space, with small mass splitting, the categories with additional leptons or Higgs boson candidates are the most sensitive.

In the SP approach, we optimize the event categorization for strong production of bottom squark pairs, which typically produce a larger number of jets and b-tagged jets. An alternative clustering algorithm is employed, following Ref. [35], to produce two hemispheres referred to as pseudojets, and the kinematic variable m_{T2} [36] is calculated as

$$m_{\mathrm{T2}} = \min_{\vec{p}_{\mathrm{T}}^{\,\mathrm{missX(1)}} + \vec{p}_{\mathrm{T}}^{\,\mathrm{missX(2)}} = \vec{p}_{\mathrm{T}}^{\,\mathrm{miss}}} \left[\max\left(m_{\mathrm{T}}^{(1)}, m_{\mathrm{T}}^{(2)} \right) \right], \tag{5}$$

where $\vec{p}_{\mathrm{T}}^{\,\mathrm{missX(i)}}$ (with i=1,2) are trial vectors obtained by decomposing $\vec{p}_{\mathrm{T}}^{\,\mathrm{miss}}$ and $m_{\mathrm{T}}^{(i)}$, the transverse masses obtained by pairing any of these trial vectors with one of the two pseudojets. The minimization is performed over all trial momenta satisfying the $\vec{p}_{\mathrm{T}}^{\,\mathrm{miss}}$ constraint. The $p_{\mathrm{T}}^{\gamma\gamma}/m_{\gamma\gamma}$ and m_{T2} kinematic variables are used to enhance the discrimination between the SUSY signal and the SM background. Two bins in the m_{T2} variable are used: $m_{\mathrm{T2}} < 30$ and $m_{\mathrm{T2}} \geq 30\,\mathrm{GeV}$; and three bins in $p_{\mathrm{T}}^{\gamma\gamma}/m_{\gamma\gamma}$: 0–0.6, 0.6–1.0 and $\geq$1.0.

Events are also separated into the Two-Lepton, Muon, Electron, $\mathrm{Hb\bar{b}}$, and $\mathrm{Zb\bar{b}}$ categories following the same procedure as described above for the EWP approach. The remaining events are separated into the hadronic categories depending on the number of jets and b-tagged jets. Within each of the event categories, the exclusive search region bins are then defined based on the values of the $p_{\mathrm{T}}^{\gamma\gamma}/m_{\gamma\gamma}$ and m_{T2} observables.

A summary of the 35 search region bins is shown in Table 1 for the EWP analysis and of the 64 search region bins in Tables 2 and 3 for the SP analysis.

Finally, to test specific SUSY simplified model hypotheses, we perform a combined simultaneous fit using all the search regions defined for each analysis. The final result for each signal model is obtained from the analysis with the best expected sensitivity. The diphoton mass distribution is fit independently in each search region, while the expected yields for the SM Higgs background and SUSY signal model among the different search regions are constrained to the predicted values.

6 Backgrounds

Two types of backgrounds can be identified for this search: a nonresonant one stemming from the SM production of diphotons or a photon and a jet, and a resonant background from SM Higgs boson production. To model the nonresonant background, a set of possible functions is chosen from sums of exponential functions, sums of Bernstein polynomials, Laurent series, and sums of power-law functions. To determine the best functional form, two alternative strategies are followed for the EWP and SP analyses. As we do not know a priori the exact shape of the background, it is important that the functional form used is capable of adequately describing a sufficiently large range of background shapes to cover potential systematic effects that affect the shapes. At the same time we do not want to arbitrarily increase the number of fit parameters without yielding additional robustness against systematic uncertainties.

The EWP analysis uses the Akaike information criterion (AIC) [37] to determine which functional forms are most appropriate to describe the background spectrum. The same procedure was employed in the previous version of this search [8]. Bias tests are performed by drawing

Table 1: A summary of the search region bins used in the EWP analysis. Events are separated into categories based on the number of leptons, the presence of $H \to b\bar{b}$ candidates, the p_T of the $H \to \gamma\gamma$ candidate, and the estimated diphoton mass resolution. The High-Res and Low-Res categories are defined by the estimated diphoton resolution mass σ_m/m being smaller or larger than 0.85%, respectively. For the Two-Lepton category, "No req." means that no requirements are placed on the given observables.

Bin number	Category	$p_T^{\gamma\gamma}$ (GeV)	M_R (GeV)	R^2
EWP 0	Two-Lepton	No req.	No req.	No req.
EWP 1	Muon High-p_T	$\geq$110	$\geq$150	$\geq$0.0
EWP 2	Muon Low-p_T	0–110	$\geq$150	$\geq$0.0
EWP 3	Electron High-p_T	$\geq$110	$\geq$150	$\geq$0.0
EWP 4	Electron Low-p_T	0–110	$\geq$150	0.000–0.055
EWP 5	Electron Low-p_T	0–110	$\geq$150	0.055–0.125
EWP 6	Electron Low-p_T	0–110	$\geq$150	$\geq$0.125
EWP 7	H$b\bar{b}$ High-p_T	$\geq$110	$\geq$150	0.000–0.080
EWP 8	H$b\bar{b}$ High-p_T	$\geq$110	$\geq$150	$\geq$0.080
EWP 9	H$b\bar{b}$ Low-p_T	0–110	$\geq$150	0.000–0.080
EWP 10	H$b\bar{b}$ Low-p_T	0–110	$\geq$150	$\geq$0.080
EWP 11	Z$b\bar{b}$ High-p_T	$\geq$110	$\geq$150	0.000–0.035
EWP 12	Z$b\bar{b}$ High-p_T	$\geq$110	$\geq$150	0.035–0.090
EWP 13	Z$b\bar{b}$ High-p_T	$\geq$110	$\geq$150	$\geq$0.090
EWP 14	Z$b\bar{b}$ Low-p_T	0–110	$\geq$150	0.000–0.035
EWP 15	Z$b\bar{b}$ Low-p_T	0–110	$\geq$150	0.035–0.090
EWP 16	Z$b\bar{b}$ Low-p_T	0–110	$\geq$150	$\geq$0.090
EWP 17	High-p_T	$\geq$110	$\geq$150	$\geq$0.260
EWP 18	High-p_T	$\geq$110	150–250	0.170–0.260
EWP 19	High-p_T	$\geq$110	$\geq$250	0.170–0.260
EWP 20	High-p_T	$\geq$110	$\geq$150	0.000–0.110
EWP 21	High-p_T	$\geq$110	150–350	0.110–0.170
EWP 22	High-p_T	$\geq$110	$\geq$350	0.110–0.170
EWP 23	High-Res	0–110	$\geq$150	$\geq$0.325
EWP 24	High-Res	0–110	$\geq$150	0.285–0.325
EWP 25	High-Res	0–110	$\geq$150	0.225–0.285
EWP 26	High-Res	0–110	$\geq$150	0.000–0.185
EWP 27	High-Res	0–110	150–200	0.185–0.225
EWP 28	High-Res	0–110	$\geq$200	0.185–0.225
EWP 29	Low-Res	0–110	$\geq$150	$\geq$0.325
EWP 30	Low-Res	0–110	$\geq$150	0.285–0.325
EWP 31	Low-Res	0–110	$\geq$150	0.225–0.285
EWP 32	Low-Res	0–110	$\geq$150	0.000–0.185
EWP 33	Low-Res	0–110	150–200	0.185–0.225
EWP 34	Low-Res	0–110	$\geq$200	0.185–0.225

random events using one functional form and fitting the resulting pseudo-data set to another functional form. The functional form with the best AIC measure passing the bias test is chosen to describe the nonresonant background.

For the SP analysis, the background fit is performed by discrete profiling using the "envelope" method [38]. The background functional form is treated as a discrete nuisance parameter in the

Table 2: A summary of the search region bins in the leptonic and Higgs boson categories used in the SP analysis, along with the requirements on $p_{\mathrm{T}}^{\gamma\gamma}/m_{\gamma\gamma}$ and m_{T2}. There are no explicit requirements on the number of jets or b-tagged jets for these categories. For the Two-Lepton category, "No req." means that no requirements are placed on the given observables.

Bin number	Bin name	Category	$p_{\mathrm{T}}^{\gamma\gamma}/m_{\gamma\gamma}$	m_{T2} (GeV)
SP 0	$\mathrm{Z}_{\ell\ell}$	Two-Lepton	No req.	No req.
SP 1	1μ p_{T}^{0}, m_{T2}^{0}	Muon	0.0–0.6	0–30
SP 2	1μ p_{T}^{0}, m_{T2}^{30}	Muon	0.0–0.6	$\geq$30
SP 3	1μ p_{T}^{75}, m_{T2}^{0}	Muon	0.6–1.0	0–30
SP 4	1μ p_{T}^{75}, m_{T2}^{30}	Muon	0.6–1.0	$\geq$30
SP 5	1μ p_{T}^{125}, m_{T2}^{0}	Muon	$\geq$1.0	0–30
SP 6	1μ p_{T}^{125}, m_{T2}^{30}	Muon	$\geq$1.0	$\geq$30
SP 7	1e p_{T}^{0}, m_{T2}^{0}	Electron	0.0–0.6	0–30
SP 8	1e p_{T}^{0}, m_{T2}^{30}	Electron	0.0–0.6	$\geq$30
SP 9	1e p_{T}^{75}, m_{T2}^{0}	Electron	0.6–1.0	0–30
SP 10	1e p_{T}^{75}, m_{T2}^{30}	Electron	0.6–1.0	$\geq$30
SP 11	1e p_{T}^{125}, m_{T2}^{0}	Electron	$\geq$1.0	0–30
SP 12	1e p_{T}^{125}, m_{T2}^{30}	Electron	$\geq$1.0	$\geq$30
SP 13	$\mathrm{Zb\bar{b}}$ p_{T}^{0}, m_{T2}^{0}	$\mathrm{Zb\bar{b}}$	0.0–0.6	0–30
SP 14	$\mathrm{Zb\bar{b}}$ p_{T}^{75}, m_{T2}^{0}	$\mathrm{Zb\bar{b}}$	0.6–1.0	0–30
SP 15	$\mathrm{Zb\bar{b}}$ p_{T}^{125}, m_{T2}^{0}	$\mathrm{Zb\bar{b}}$	$\geq$1.0	0–30
SP 16	$\mathrm{Zb\bar{b}}$ p_{T}^{0}, m_{T2}^{30}	$\mathrm{Zb\bar{b}}$	0.0–0.6	$\geq$30
SP 17	$\mathrm{Zb\bar{b}}$ p_{T}^{75}, m_{T2}^{30}	$\mathrm{Zb\bar{b}}$	0.6–1.0	$\geq$30
SP 18	$\mathrm{Zb\bar{b}}$ p_{T}^{125}, m_{T2}^{30}	$\mathrm{Zb\bar{b}}$	$\geq$1.0	$\geq$30
SP 19	$\mathrm{Hb\bar{b}}$ p_{T}^{0}, m_{T2}^{0}	$\mathrm{Hb\bar{b}}$	0.0–0.6	0–30
SP 20	$\mathrm{Hb\bar{b}}$ p_{T}^{75}, m_{T2}^{0}	$\mathrm{Hb\bar{b}}$	0.6–1.0	0–30
SP 21	$\mathrm{Hb\bar{b}}$ p_{T}^{125}, m_{T2}^{0}	$\mathrm{Hb\bar{b}}$	$\geq$1.0	0–30
SP 22	$\mathrm{Hb\bar{b}}$ p_{T}^{0}, m_{T2}^{30}	$\mathrm{Hb\bar{b}}$	0.0–0.6	$\geq$30
SP 23	$\mathrm{Hb\bar{b}}$ p_{T}^{75}, m_{T2}^{30}	$\mathrm{Hb\bar{b}}$	0.6–1.0	$\geq$30
SP 24	$\mathrm{Hb\bar{b}}$ p_{T}^{125}, m_{T2}^{30}	$\mathrm{Hb\bar{b}}$	$\geq$1.0	$\geq$30

likelihood fit. A penalty is assigned to the likelihood for each parameter in the function. The envelope with the best likelihood is determined by the discrete profiling method taking penalties into account. Similar accuracy is expected of the two alternative background fit methods.

7 Systematic uncertainties

The dominant systematic uncertainties in this search are the shape and normalization of the nonresonant background, propagated by profiling the associated unconstrained parameters. The subdominant systematic uncertainties in the SM Higgs boson background and SUSY signal are propagated through independent log-normal nuisance parameters that take both theoretical and instrumental effects into account. These systematic uncertainties affect the event yield predictions of the SM Higgs boson background and SUSY signal in the different search region bins, and are propagated as shape uncertainties. The independent systematic effects considered include missing higher-order QCD corrections, PDFs, trigger and object selection efficiencies, jet energy scale uncertainties, b-tagging efficiency, lepton identification efficiencies, fast simulation $p_{\mathrm{T}}^{\mathrm{miss}}$ modeling, and the uncertainty in the integrated luminosity. The typical

Table 3: A summary of the search region bins in the leptonic and Higgs boson categories used in the SP analysis, along with the requirements on $p_{\mathrm{T}}^{\gamma\gamma}/m_{\gamma\gamma}$ and m_{T2}. "No req." means that no requirements are placed on the given observables.

Bin number	Bin name	Jets	b-tagged jets	$p_{\mathrm{T}}^{\gamma\gamma}/m_{\gamma\gamma}$	m_{T2} (GeV)
SP 25	0j, $\geq$0b, p_{T}^{0}	0	No req.	0.0–0.6	No req.
SP 26	0j, $\geq$0b, p_{T}^{75}	0	No req.	0.6–1.0	No req.
SP 27	0j, $\geq$0b, p_{T}^{125}	0	No req.	$\geq$1.0	No req.
SP 28	1–3j, 0b, p_{T}^{0}, m_{T2}^{0}	1–3	0	0.0–0.6	0–30
SP 29	1–3j, 0b, p_{T}^{0}, m_{T2}^{30}	1–3	0	0.0–0.6	$\geq$30
SP 30	1–3j, 0b, p_{T}^{75}, m_{T2}^{0}	1–3	0	0.6–1.0	0–30
SP 31	1–3j, 0b, p_{T}^{75}, m_{T2}^{30}	1–3	0	0.6–1.0	$\geq$30
SP 32	1–3j, 0b, p_{T}^{125}, m_{T2}^{0}	1–3	0	$\geq$1.0	0–30
SP 33	1–3j, 0b, p_{T}^{125}, m_{T2}^{30}	1–3	0	$\geq$1.0	$\geq$30
SP 34	1–3j, 1b, p_{T}^{0}, m_{T2}^{0}	1–3	1	0.0–0.6	0–30
SP 35	1–3j, 1b, p_{T}^{0}, m_{T2}^{30}	1–3	1	0.0–0.6	$\geq$30
SP 36	1–3j, 1b, p_{T}^{75}, m_{T2}^{0}	1–3	1	0.6–1.0	0–30
SP 37	1–3j, 1b, p_{T}^{75}, m_{T2}^{30}	1–3	1	0.6–1.0	$\geq$30
SP 38	1–3j, 1b, p_{T}^{125}, m_{T2}^{0}	1–3	1	$\geq$1.0	0–30
SP 39	1–3j, 1b, p_{T}^{125}, m_{T2}^{30}	1–3	1	$\geq$1.0	$\geq$30
SP 40	1–3j, $\geq$2b, p_{T}^{0}, m_{T2}^{0}	1–3	$\geq$2	0.0–0.6	0–30
SP 41	1–3j, $\geq$2b, p_{T}^{0}, m_{T2}^{30}	1–3	$\geq$2	0.0–0.6	$\geq$30
SP 42	1–3j, $\geq$2b, p_{T}^{75}, m_{T2}^{0}	1–3	$\geq$2	0.6–1.0	0–30
SP 43	1–3j, $\geq$2b, p_{T}^{75}, m_{T2}^{30}	1–3	$\geq$2	0.6–1.0	$\geq$30
SP 44	1–3j, $\geq$2b, p_{T}^{125}, m_{T2}^{0}	1–3	$\geq$2	$\geq$1.0	0–30
SP 45	1–3j, $\geq$2b, p_{T}^{125}, m_{T2}^{30}	1–3	$\geq$2	$\geq$1.0	$\geq$30
SP 46	$\geq$4j, 0b, p_{T}^{0}, m_{T2}^{0}	$\geq$4	0	0.0–0.6	0–30
SP 47	$\geq$4j, 0b, p_{T}^{0}, m_{T2}^{30}	$\geq$4	0	0.0–0.6	$\geq$30
SP 48	$\geq$4j, 0b, p_{T}^{75}, m_{T2}^{0}	$\geq$4	0	0.6–1.0	0–30
SP 49	$\geq$4j, 0b, p_{T}^{75}, m_{T2}^{30}	$\geq$4	0	0.6–1.0	$\geq$30
SP 50	$\geq$4j, 0b, p_{T}^{125}, m_{T2}^{0}	$\geq$4	0	$\geq$1.0	0–30
SP 51	$\geq$4j, 0b, p_{T}^{125}, m_{T2}^{30}	$\geq$4	0	$\geq$1.0	$\geq$30
SP 52	$\geq$4j, 1b, p_{T}^{0}, m_{T2}^{0}	$\geq$4	1	0.0–0.6	0–30
SP 53	$\geq$4j, 1b, p_{T}^{0}, m_{T2}^{30}	$\geq$4	1	0.0–0.6	$\geq$30
SP 54	$\geq$4j, 1b, p_{T}^{75}, m_{T2}^{0}	$\geq$4	1	0.6–1.0	0–30
SP 55	$\geq$4j, 1b, p_{T}^{75}, m_{T2}^{30}	$\geq$4	1	0.6–1.0	$\geq$30
SP 56	$\geq$4j, 1b, p_{T}^{125}, m_{T2}^{0}	$\geq$4	1	$\geq$1.0	0–30
SP 57	$\geq$4j, 1b, p_{T}^{125}, m_{T2}^{30}	$\geq$4	1	$\geq$1.0	$\geq$30
SP 58	$\geq$4j, $\geq$2b, p_{T}^{0}, m_{T2}^{0}	$\geq$4	$\geq$2	0.0–0.6	0–30
SP 59	$\geq$4j, $\geq$2b, p_{T}^{0}, m_{T2}^{30}	$\geq$4	$\geq$2	0.0–0.6	$\geq$30
SP 60	$\geq$4j, $\geq$2b, p_{T}^{75}, m_{T2}^{0}	$\geq$4	$\geq$2	0.6–1.0	0–30
SP 61	$\geq$4j, $\geq$2b, p_{T}^{75}, m_{T2}^{30}	$\geq$4	$\geq$2	0.6–1.0	$\geq$30
SP 62	$\geq$4j, $\geq$2b, p_{T}^{125}, m_{T2}^{0}	$\geq$4	$\geq$2	$\geq$1.0	0–30
SP 63	$\geq$4j, $\geq$2b, p_{T}^{125}, m_{T2}^{30}	$\geq$4	$\geq$2	$\geq$1.0	$\geq$30

size of these effects on the signal and background yields are summarized in Table 4, and are approximately the same for the SP and EWP analyses. Systematic uncertainties due to missing higher-order corrections are estimated by the use of the procedure outlined in Ref. [39], where

the factorization (μ_F) and renormalization (μ_R) scales are varied independently by factors of 0.5 and 2.0. The PDF systematic uncertainties are propagated for the SM Higgs background as a shape uncertainty using the LHC4PDF procedure [40].

Because of the imperfect simulation of the effects of pileup and transparency loss from radiation damage in the ECAL crystals, we observe some simulation mismodeling of the estimated mass resolution, which can migrate events between the High-Res and Low-Res event categories of the EWP analysis. As a result, a systematic uncertainty of 10–24%, measured using a $Z \to e^+e^-$ control sample, is propagated to the prediction of the SM Higgs boson background and SUSY signal yields in the High-Res and Low-Res event categories. The systematic uncertainty in the photon energy scale is implemented as a Gaussian-distributed nuisance parameter that shifts the Higgs boson mass peak position, constrained in the fit to lie within approximately 1% of the nominal Higgs boson mass observed in simulation. The systematic uncertainty for the modeling of the ISR for the signal process is also propagated.

Table 4: Summary of systematic uncertainties on the SM Higgs boson background and signal yield predictions, and the size of their effect on the signal yield.

Uncertainty source	Uncertainty size (%)
PDFs and QCD scale variations	15–30
Signal ISR modeling	25
σ_m/m categorization	10–24
Fast simulation p_T^{miss} modeling	3–16
Luminosity	2.3–2.5
Trigger and selection efficiency	3
Lepton efficiency	4
Jet energy scale	1–5
Photon energy scale	1
b-tagging efficiency	4
$H \to \gamma\gamma$ branching fraction	2

8 Results and interpretation

The fit results for the search region bins including the data yields, fitted background, and signal yields are summarized in Tables 5 and 6 for the SP analysis and in Table 7 for the EWP analysis. One example fit result is shown in Fig. 2 to illustrate the background-only and signal plus background fits. We observe no statistically significant deviation from the SM background expectation.

The search result is interpreted in terms of limits on the product of the production cross section and branching fraction for simplified models of bottom squark pair production and chargino-neutralino production indicated in Fig. 1. In the case of bottom squark pair production, we consider the scenario where the bottom squark subsequently decays to a bottom quark and the next-to-lightest neutralino ($\widetilde{\chi}_2^0$), where the $\widetilde{\chi}_2^0$ decays to a Higgs boson and the LSP ($\widetilde{\chi}_1^0$). The production cross sections are computed at NLO plus next-to-leading logarithmic (NLL) accuracy in QCD [41–46] under the assumption that all SUSY particles other than those in the relevant diagram are too heavy to participate in the interaction. We consider scenarios where the mass splitting between the $\widetilde{\chi}_2^0$ and $\widetilde{\chi}_1^0$ is 130 GeV, slightly above threshold to produce an on-shell Higgs boson.

In the case of chargino-neutralino production, we consider two different scenarios. In the first scenario, the pure wino-like charginos ($\widetilde{\chi}_1^\pm$) and the $\widetilde{\chi}_2^0$ are mass-degenerate and are produced

Table 5: The observed data, fitted nonresonant background yields, and SM Higgs boson background yields within the mass window between 122 and 129 GeV are shown for each search region bin in the $\mathrm{Hb\bar{b}}$, $\mathrm{Zb\bar{b}}$, and leptonic categories of the SP analysis. The uncertainties quoted are the fit uncertainties, which include the impact of all systematic uncertainties. The bin names give a short-form description of the search region bin definition which are given in full in Table 2. The labels p_{T}^{0}, p_{T}^{75}, and p_{T}^{125} refer to bins defined by the requirement that $p_{\mathrm{T}}^{\gamma\gamma}/m_{\gamma\gamma}$ is less than 0.6, between 0.6 and 1.0, and greater than 1.0, respectively. The labels m_{T2}^{0} and m_{T2}^{30} refer to bins defined by the requirement that m_{T2} is less than and greater than 30 GeV, respectively.

Search region bin	Bin name	Observed data	Fitted nonresonant bkg	SM Higgs boson bkg
SP 0	$\mathrm{Z}_{\ell\ell}$	2	1.7 ± 0.2	0.84 ± 0.09
SP 1	1μ p_{T}^{0}, m_{T2}^{0}	24	20.0 ± 0.9	1.6 ± 0.1
SP 2	1μ p_{T}^{0}, m_{T2}^{30}	10	8.9 ± 1.4	1.1 ± 0.1
SP 3	1μ p_{T}^{75}, m_{T2}^{0}	3	2.6 ± 0.5	0.89 ± 0.07
SP 4	1μ p_{T}^{75}, m_{T2}^{30}	7	2.4 ± 0.4	0.79 ± 0.07
SP 5	1μ p_{T}^{125}, m_{T2}^{0}	4	3.1 ± 0.4	1.0 ± 0.1
SP 6	1μ p_{T}^{125}, m_{T2}^{30}	3	2.2 ± 0.4	1.1 ± 0.1
SP 7	1e p_{T}^{0}, m_{T2}^{0}	93	87.2 ± 10.6	1.1 ± 0.1
SP 8	1e p_{T}^{0}, m_{T2}^{30}	15	13.8 ± 0.9	0.59 ± 0.05
SP 9	1e p_{T}^{75}, m_{T2}^{0}	10	18.6 ± 3.0	0.74 ± 0.06
SP 10	1e p_{T}^{75}, m_{T2}^{30}	3	4.3 ± 0.3	0.48 ± 0.04
SP 11	1e p_{T}^{125}, m_{T2}^{0}	7	6.2 ± 0.4	1.1 ± 0.1
SP 12	1e p_{T}^{125}, m_{T2}^{30}	1	1.4 ± 0.2	0.89 ± 0.08
SP 13	$\mathrm{Zb\bar{b}}$ p_{T}^{0}, m_{T2}^{0}	227	224 ± 17	4.4 ± 0.6
SP 14	$\mathrm{Zb\bar{b}}$ p_{T}^{75}, m_{T2}^{0}	33	42.2 ± 7.4	1.7 ± 0.2
SP 15	$\mathrm{Zb\bar{b}}$ p_{T}^{125}, m_{T2}^{0}	15	15.7 ± 3.6	2.9 ± 0.3
SP 16	$\mathrm{Zb\bar{b}}$ p_{T}^{0}, m_{T2}^{30}	44	43.4 ± 7.5	0.83 ± 0.40
SP 17	$\mathrm{Zb\bar{b}}$ p_{T}^{75}, m_{T2}^{30}	13	10.8 ± 2.3	0.48 ± 0.13
SP 18	$\mathrm{Zb\bar{b}}$ p_{T}^{125}, m_{T2}^{30}	5	4.5 ± 0.4	0.82 ± 0.11
SP 19	$\mathrm{Hb\bar{b}}$ p_{T}^{0}, m_{T2}^{0}	179	179 ± 15	3.4 ± 0.3
SP 20	$\mathrm{Hb\bar{b}}$ p_{T}^{75}, m_{T2}^{0}	45	41.2 ± 1.9	1.9 ± 0.2
SP 21	$\mathrm{Hb\bar{b}}$ p_{T}^{125}, m_{T2}^{0}	22	18.4 ± 1.8	3.0 ± 0.9
SP 22	$\mathrm{Hb\bar{b}}$ p_{T}^{0}, m_{T2}^{30}	47	42.5 ± 7.4	0.93 ± 0.32
SP 23	$\mathrm{Hb\bar{b}}$ p_{T}^{75}, m_{T2}^{30}	13	12.1 ± 0.8	0.62 ± 0.06
SP 24	$\mathrm{Hb\bar{b}}$ p_{T}^{125}, m_{T2}^{30}	6	4.4 ± 0.7	1.3 ± 0.2

together, with the chargino decaying to a W boson and the $\widetilde{\chi}_1^0$ LSP, and the $\widetilde{\chi}_2^0$ decaying to a Higgs boson and the LSP. The production cross sections are computed at NLO+NLL accuracy in QCD in the limit of mass-degenerate wino $\widetilde{\chi}_2^0$ and $\widetilde{\chi}_1^{\pm}$, light bino $\widetilde{\chi}_1^0$, and with all the other sparticles assumed to be heavy and decoupled [47–49].

In the second scenario, we consider a GMSB [4, 5] simplified model where higgsino-like charginos and neutralinos are nearly mass-degenerate and are produced in pairs through the following combinations: $\widetilde{\chi}_1^0\widetilde{\chi}_2^0$, $\widetilde{\chi}_1^0\widetilde{\chi}_1^{\pm}$, $\widetilde{\chi}_2^0\widetilde{\chi}_1^{\pm}$, and $\widetilde{\chi}_1^{\pm}\widetilde{\chi}_1^{\mp}$. Because of the mass degeneracy, both the $\widetilde{\chi}_2^0$ and $\widetilde{\chi}_1^{\pm}$ will decay to $\widetilde{\chi}_1^0$ and other low-p_{T} (soft) particles, leading to a signature with a $\widetilde{\chi}_1^0$ pair. Each $\widetilde{\chi}_1^0$ will subsequently decay to a Higgs boson and the $\widetilde{\mathrm{G}}$ LSP, or to a Z boson and the LSP. We consider the case where the branching fraction of the $\widetilde{\chi}_1^0 \to \mathrm{H}\widetilde{\mathrm{G}}$ decay is 100%,

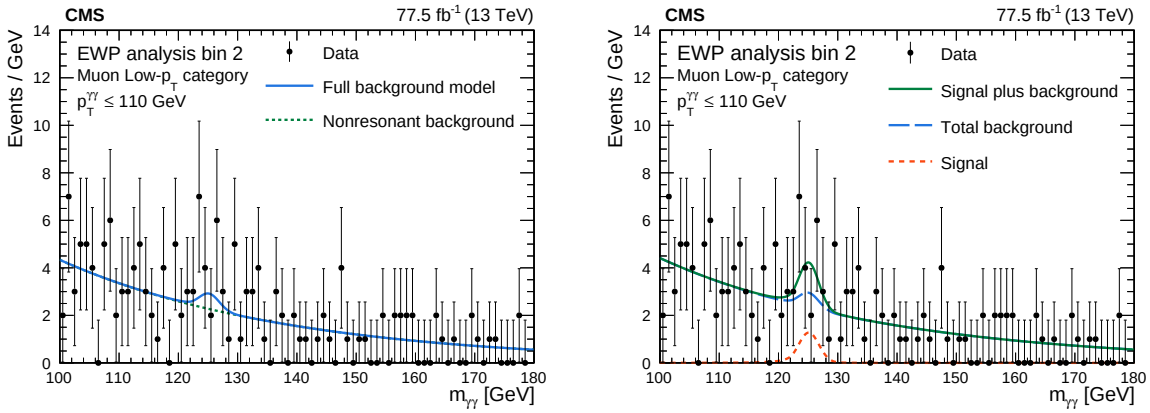

Figure 2: The diphoton mass distribution for one example search bin is shown with the background-only fit (left) and the signal-plus-background fit (right) to illustrate the signal extraction procedure. The search region bin shown corresponds to the Muon Low-p_{T} category (bin 2) of the EWP analysis.

and the case where the branching fraction of the $\widetilde{\chi}_1^0 \to \mathrm{H}\widetilde{\mathrm{G}}$ and $\widetilde{\chi}_1^0 \to \mathrm{Z}\widetilde{\mathrm{G}}$ decays are each 50%. This scenario is represented by the $\widetilde{\chi}_1^0$-pair production simplified model shown on Fig. 1. The cross sections for higgsino pair production are computed at NLO+NLL precision in the limit of mass-degenerate higgsinos $\widetilde{\chi}_2^0$, $\widetilde{\chi}_1^{\pm}$, and $\widetilde{\chi}_1^0$, with all the other sparticles assumed to be heavy and decoupled [47–49]. Following the convention of real mixing matrices and signed neutralino or chargino masses [50], we set the mass of $\widetilde{\chi}_1^0$ ($\widetilde{\chi}_2^0$) to positive (negative) values. The product of the third and fourth elements of the corresponding rows of the neutralino mixing matrix N is $+0.5$ (-0.5). The elements U_{12} and V_{12} of the chargino mixing matrices are set to 1.

We show the expected event yields from a representative selection of the different simplified SUSY models considered in the different search region bins of the SP analysis in Tables 8 and 9, and in the different search region bins of the EWP analysis in Table 10. The details of the particular signal model are described in the caption of Table 8.

Following the $\mathrm{CL_s}$ criterion [51–53], we use the profile likelihood ratio test statistic and the asymptotic formula [54] to evaluate the 95% confidence level (CL) observed and expected limits on the signal production cross sections. For the simplified models of bottom squark pair production where the bottom squark undergoes a cascade decay to a Higgs boson and the LSP, the SP analysis yields better expected sensitivity because of the binning in the number of jets and b-tagged jets, as more jets and more heavy-flavor jets are produced. The limits obtained using the SP analysis are shown in Fig. 3, as a function of the bottom squark mass and the LSP mass. We exclude bottom squarks with masses below about 530 GeV for an LSP mass of 1 GeV.

For the simplified models of chargino-neutralino production, the EWP analysis has slightly better expected sensitivity because of the inclusion of bins with smaller M_{R} and larger R^2. Events in such bins typically have lower values of $p_{\mathrm{T}}^{\mathrm{miss}}$ and are not in the regions of high signal sensitivity for the SP analysis, while the R^2 variable is able to suppress backgrounds more effectively in these regions of phase space. For the wino-like chargino-neutralino production, the limits obtained using the EWP analysis are shown in Fig. 4 as a function of the chargino mass and the LSP mass. We exclude chargino masses below about 235 GeV for an LSP mass of 1 GeV. For the higgsino-like chargino-neutralino production simplified models, the limits obtained using the EWP analysis are shown in Fig. 5 as a function of the chargino mass for the case where the branching fraction of the $\widetilde{\chi}_1^0 \to \mathrm{H}\widetilde{\mathrm{G}}$ decay is 100%, and for the case where the branching fraction of the $\widetilde{\chi}_1^0 \to \mathrm{H}\widetilde{\mathrm{G}}$ and $\widetilde{\chi}_1^0 \to \mathrm{Z}\widetilde{\mathrm{G}}$ decays are both 50%. We exclude charginos below 290

and 230 GeV in the former and latter cases, respectively.

The corresponding limits from the EWP analysis as applied to bottom squark production and limits from the SP analysis as applied to chargino-neutralino production are included in the appendix for completeness.

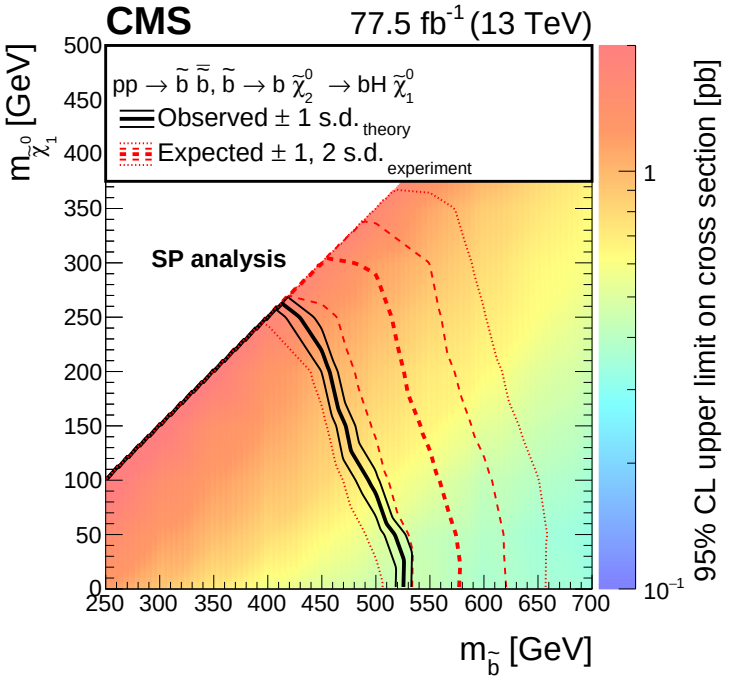

Figure 3: The observed 95% CL upper limits on the bottom squark pair production cross section are shown for the SP analysis. The bold and light solid black contours represent the observed exclusion region and the ± 1 standard deviation (s.d.) band, including both experimental and theoretical uncertainties. The analogous red dotted contours represent the expected exclusion region and its ± 1 and ± 2 s.d. bands.

9 Summary

We have presented a search for supersymmetry (SUSY) in the final state with a Higgs boson (H) decaying to a photon pair, using data collected with the CMS detector at the LHC in 2016 and 2017, corresponding to 77.5 fb^{-1} of integrated luminosity. To improve the sensitivity over previously published results, we pursue two complementary strategies that are optimized for strong and electroweak SUSY production, respectively. Photon pairs in the central region of the detector are used to reconstruct Higgs boson candidates. Charged leptons and b jets are used to tag the decay products of an additional boson, while kinematic quantities such as m_{T2} and the razor variables M_{R} and R^2 are used to suppress standard model backgrounds. Data driven fits determine the shape of the nonresonant background. The resonant background from standard model Higgs boson production is estimated from simulation. The results are interpreted in terms of exclusion limits on the production cross section of simplified models of bottom squark pair production and chargino-neutralino production. As a result of the improvements in the event categorization and the larger data set, we extend the mass limits over the previous best results [8, 9] by about 100 GeV for bottom squark pair production and about 50 GeV for chargino-neutralino production. We exclude bottom squark pair production for bottom squark masses below 530 GeV for a lightest SUSY particle (LSP) mass of 1 GeV; wino-like chargino-

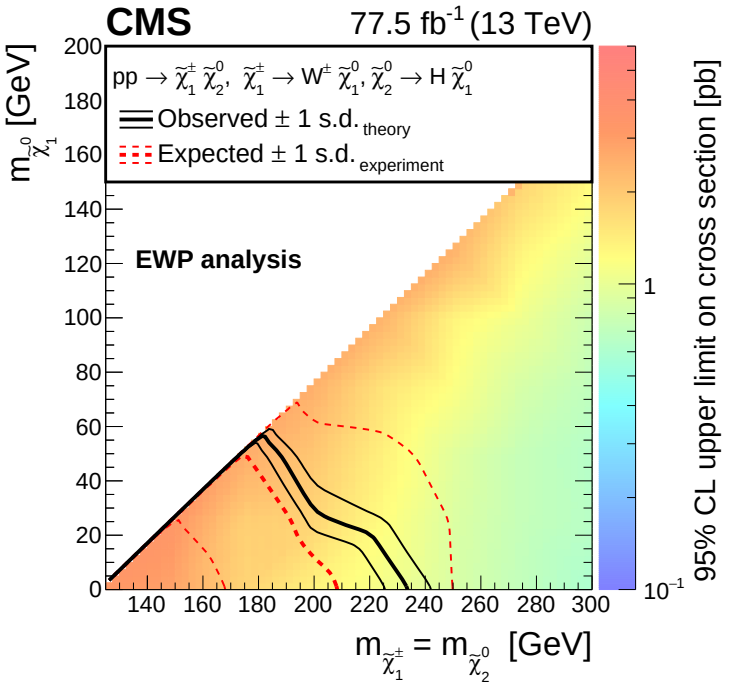

Figure 4: The observed 95% CL upper limits on the wino-like chargino-neutralino production cross section are shown for the EWP analysis. The bold and light black contours represent the observed exclusion region and the ± 1 standard deviation (s.d.) band, including both experimental and theoretical uncertainties. The analogous red dotted contours represent the expected exclusion region and its ± 1 s.d. band.

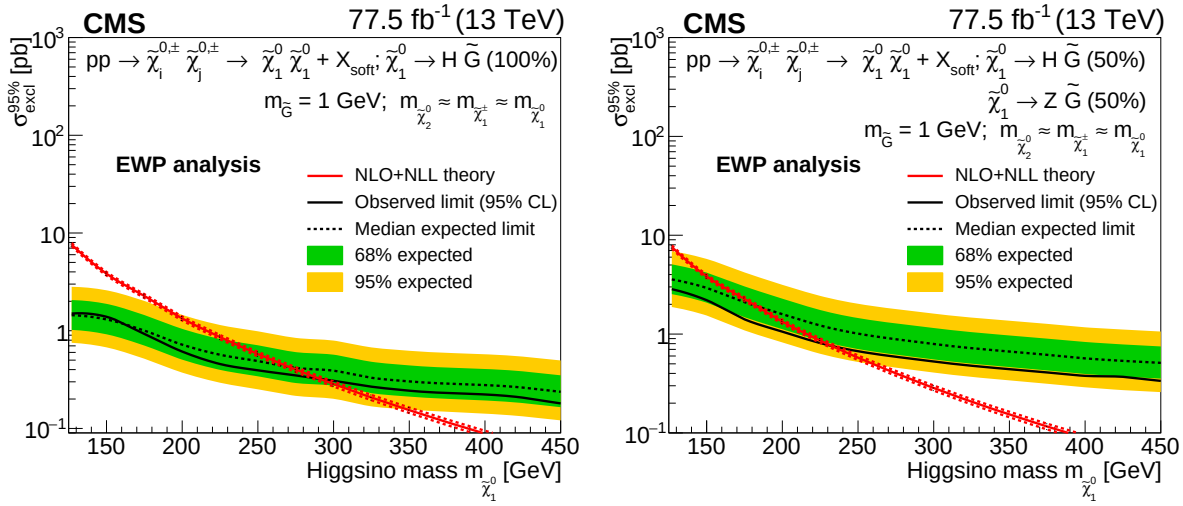

Figure 5: The observed 95% CL upper limits on the production cross section for higgsino-like chargino-neutralino production are shown for the EWP analysis. We present limits in the scenario where the branching fraction of $\widetilde{\chi}_1^0 \to \mathrm{H}\widetilde{\mathrm{G}}$ decay is 100% (left plot), and where the $\widetilde{\chi}_1^0 \to \mathrm{H}\widetilde{\mathrm{G}}$ and $\widetilde{\chi}_1^0 \to \mathrm{Z}\widetilde{\mathrm{G}}$ decays are each 50% (right plot). The dotted and solid black curves represent the expected and observed exclusion region, and the green dark and yellow light bands represent the ± 1 and ± 2 standard deviation regions, respectively. The red solid and dotted lines show the theoretical production cross section and its uncertainty band.

neutralino production, for chargino and neutralino masses of up to 235 GeV and an LSP mass of 1 GeV; and higgsino-like chargino-neutralino production, for chargino and neutralino masses of up to 290 and 230 GeV for the cases where the branching fraction of the lightest neutralino $\widetilde{\chi}_1^0 \to \mathrm{H}\widetilde{\mathrm{G}}$ decay is 100%, and where the branching fractions of the $\widetilde{\chi}_1^0 \to \mathrm{H}\widetilde{\mathrm{G}}$ and $\widetilde{\chi}_1^0 \to \mathrm{Z}\widetilde{\mathrm{G}}$ decays are both 50%, respectively.

Table 6: The observed data, fitted nonresonant background yields, and SM Higgs boson background yields within the mass window between 122 and 129 GeV are shown for each search region bin in the all-hadronic categories of the SP analysis. The uncertainties quoted are the fit uncertainties, which include the impact of all systematic uncertainties. The bin names give a short-form description of the search region bin definition which are given in full in Table 3. The labels p_{T}^{0}, p_{T}^{75}, and p_{T}^{125} refer to bins defined by the requirement that $p_{\mathrm{T}}^{\gamma\gamma}/m_{\gamma\gamma}$ is less than 0.6, between 0.6 and 1.0, and greater than 1.0, respectively. The labels m_{T2}^{0} and m_{T2}^{30} refer to bins defined by the requirement that m_{T2} is less than and greater than 30 GeV, respectively.

Search region bin	Bin name	Observed data	Fitted nonresonant bkg	SM Higgs boson bkg
SP 25	0j, $\geq$0b, p_{T}^{0}	53 252	53 662 $\pm$ 104	973 $\pm$ 68
SP 26	0j, $\geq$0b, p_{T}^{75}	586	574 $\pm$ 27	33.3 $\pm$ 4.1
SP 27	0j, $\geq$0b, p_{T}^{125}	51	49.5 $\pm$ 8.0	7.4 $\pm$ 0.8
SP 28	1–3j, 0b, p_{T}^{0}, m_{T2}^{0}	14 648	14 753 $\pm$ 138	308 $\pm$ 33
SP 29	1–3j, 0b, p_{T}^{0}, m_{T2}^{30}	2732	2725 $\pm$ 10	125 $\pm$ 10
SP 30	1–3j, 0b, p_{T}^{75}, m_{T2}^{0}	781	708 $\pm$ 30	101 $\pm$ 9
SP 31	1–3j, 0b, p_{T}^{75}, m_{T2}^{30}	103	101 $\pm$ 11	0.90 $\pm$ 0.38
SP 32	1–3j, 0b, p_{T}^{125}, m_{T2}^{0}	47	46.6 $\pm$ 7.7	0.95 $\pm$ 0.28
SP 33	1–3j, 0b, p_{T}^{125}, m_{T2}^{30}	52	37.2 $\pm$ 6.9	3.9 $\pm$ 0.6
SP 34	1–3j, 1b, p_{T}^{0}, m_{T2}^{0}	4184	4149 $\pm$ 7	78.4 $\pm$ 7.7
SP 35	1–3j, 1b, p_{T}^{0}, m_{T2}^{30}	928	902 $\pm$ 34	35.3 $\pm$ 3.1
SP 36	1–3j, 1b, p_{T}^{75}, m_{T2}^{0}	273	270 $\pm$ 19	36.4 $\pm$ 3.1
SP 37	1–3j, 1b, p_{T}^{75}, m_{T2}^{30}	75	78.0 $\pm$ 10.0	1.3 $\pm$ 0.1
SP 38	1–3j, 1b, p_{T}^{125}, m_{T2}^{0}	52	43.7 $\pm$ 7.5	0.97 $\pm$ 0.26
SP 39	1–3j, 1b, p_{T}^{125}, m_{T2}^{30}	38	30.8 $\pm$ 6.3	3.7 $\pm$ 0.8
SP 40	1–3j, $\geq$2b, p_{T}^{0}, m_{T2}^{0}	312	292 $\pm$ 19	5.6 $\pm$ 0.8
SP 41	1–3j, $\geq$2b, p_{T}^{0}, m_{T2}^{30}	79	79.6 $\pm$ 10.1	3.0 $\pm$ 0.3
SP 42	1–3j, $\geq$2b, p_{T}^{75}, m_{T2}^{0}	37	34.3 $\pm$ 6.6	4.5 $\pm$ 0.6
SP 43	1–3j, $\geq$2b, p_{T}^{75}, m_{T2}^{30}	26	24.0 $\pm$ 5.6	0.57 $\pm$ 0.06
SP 44	1–3j, $\geq$2b, p_{T}^{125}, m_{T2}^{0}	16	12.3 $\pm$ 0.8	0.54 $\pm$ 0.10
SP 45	1–3j, $\geq$2b, p_{T}^{125}, m_{T2}^{30}	15	10.0 $\pm$ 0.8	1.7 $\pm$ 0.2
SP 46	$\geq$4j, 0b, p_{T}^{0}, m_{T2}^{0}	2429	2426 $\pm$ 7	35.3 $\pm$ 2.6
SP 47	$\geq$4j, 0b, p_{T}^{0}, m_{T2}^{30}	339	339 $\pm$ 21	12.9 $\pm$ 1.2
SP 48	$\geq$4j, 0b, p_{T}^{75}, m_{T2}^{0}	118	97.8 $\pm$ 11.2	11.1 $\pm$ 2.2
SP 49	$\geq$4j, 0b, p_{T}^{75}, m_{T2}^{30}	15	19.5 $\pm$ 3.1	0.16 $\pm$ 0.05
SP 50	$\geq$4j, 0b, p_{T}^{125}, m_{T2}^{0}	13	10.0 $\pm$ 1.7	0.08 $\pm$ 1.76
SP 51	$\geq$4j, 0b, p_{T}^{125}, m_{T2}^{30}	7	6.5 $\pm$ 0.6	0.73 $\pm$ 0.18
SP 52	$\geq$4j, 1b, p_{T}^{0}, m_{T2}^{0}	833	800 $\pm$ 32	12.3 $\pm$ 2.5
SP 53	$\geq$4j, 1b, p_{T}^{0}, m_{T2}^{30}	132	135 $\pm$ 13	4.6 $\pm$ 0.3
SP 54	$\geq$4j, 1b, p_{T}^{75}, m_{T2}^{0}	33	42.5 $\pm$ 7.4	4.8 $\pm$ 0.7
SP 55	$\geq$4j, 1b, p_{T}^{75}, m_{T2}^{30}	13	20.2 $\pm$ 5.1	0.35 $\pm$ 0.04
SP 56	$\geq$4j, 1b, p_{T}^{125}, m_{T2}^{0}	10	11.4 $\pm$ 1.5	0.34 $\pm$ 0.04
SP 57	$\geq$4j, 1b, p_{T}^{125}, m_{T2}^{30}	9	8.4 $\pm$ 0.6	0.97 $\pm$ 0.11
SP 58	$\geq$4j, $\geq$2b, p_{T}^{0}, m_{T2}^{0}	90	88.4 $\pm$ 10.7	1.1 $\pm$ 0.3
SP 59	$\geq$4j, $\geq$2b, p_{T}^{0}, m_{T2}^{30}	25	20.9 $\pm$ 4.6	0.52 $\pm$ 0.06
SP 60	$\geq$4j, $\geq$2b, p_{T}^{75}, m_{T2}^{0}	11	8.7 $\pm$ 0.6	0.84 $\pm$ 0.17
SP 61	$\geq$4j, $\geq$2b, p_{T}^{75}, m_{T2}^{30}	12	11.5 $\pm$ 3.7	0.26 $\pm$ 0.09
SP 62	$\geq$4j, $\geq$2b, p_{T}^{125}, m_{T2}^{0}	6	3.7 $\pm$ 0.4	0.24 $\pm$ 0.08
SP 63	$\geq$4j, $\geq$2b, p_{T}^{125}, m_{T2}^{30}	4	5.2 $\pm$ 1.1	0.69 $\pm$ 0.09

Table 7: The observed data, fitted nonresonant background yields, and SM Higgs boson background yields within the mass window between 122 and 129 GeV are shown for each search region bin of the EWP analysis. The uncertainties quoted are the fit uncertainties, which include the impact of all systematic uncertainties.

Search region bin	Category	Observed data	Fitted nonresonant bkg	SM Higgs boson bkg
EWP 0	Two-Lepton	2	1.5 ± 0.4	1.1 ± 0.6
EWP 1	Muon High-p_{T}	11	6.2 ± 0.9	3.7 ± 0.8
EWP 2	Muon Low-p_{T}	28	15.8 ± 1.4	3.0 ± 0.8
EWP 3	Electron High-p_{T}	17	11.9 ± 1.3	3.4 ± 1.1
EWP 4	Electron Low-p_{T}	8	5.2 ± 0.8	0.6 ± 0.2
EWP 5	Electron Low-p_{T}	18	31.5 ± 1.9	0.9 ± 0.4
EWP 6	Electron Low-p_{T}	9	13.7 ± 1.3	0.7 ± 0.3
EWP 7	$\mathrm{Hb\bar{b}}$ High-p_{T}	9	7.0 ± 0.9	1.2 ± 0.4
EWP 8	$\mathrm{Hb\bar{b}}$ High-p_{T}	19	17.8 ± 1.5	3.8 ± 0.7
EWP 9	$\mathrm{Hb\bar{b}}$ Low-p_{T}	34	25.8 ± 1.8	0.8 ± 0.1
EWP 10	$\mathrm{Hb\bar{b}}$ Low-p_{T}	60	51.0 ± 2.4	1.9 ± 0.3
EWP 11	$\mathrm{Zb\bar{b}}$ High-p_{T}	3	7.2 ± 1.1	0.5 ± 0.1
EWP 12	$\mathrm{Zb\bar{b}}$ High-p_{T}	17	14.0 ± 1.3	2.8 ± 1.1
EWP 13	$\mathrm{Zb\bar{b}}$ High-p_{T}	10	9.4 ± 1.1	1.3 ± 0.3
EWP 14	$\mathrm{Zb\bar{b}}$ Low-p_{T}	27	35.2 ± 2.0	0.8 ± 0.2
EWP 15	$\mathrm{Zb\bar{b}}$ Low-p_{T}	84	75.1 ± 2.9	2.5 ± 1.3
EWP 16	$\mathrm{Zb\bar{b}}$ Low-p_{T}	45	46.3 ± 2.3	1.2 ± 0.4
EWP 17	High-p_{T}	11	14.4 ± 1.3	1.8 ± 0.2
EWP 18	High-p_{T}	31	21.8 ± 1.6	2.1 ± 0.4
EWP 19	High-p_{T}	11	13.5 ± 1.3	1.2 ± 0.3
EWP 20	High-p_{T}	1834	1648 ± 14	248 ± 38
EWP 21	High-p_{T}	91	100.2 ± 3.7	8.9 ± 1.5
EWP 22	High-p_{T}	12	14.4 ± 1.4	1.2 ± 0.2
EWP 23	High-Res	30	20.6 ± 1.6	0.6 ± 0.2
EWP 24	High-Res	46	49.1 ± 4.0	1.5 ± 0.5
EWP 25	High-Res	9	17.0 ± 1.4	0.4 ± 0.1
EWP 26	High-Res	5186	5057 ± 25	219 ± 42
EWP 27	High-Res	53	63.0 ± 2.6	2.4 ± 1.0
EWP 28	High-Res	19	17.7 ± 1.5	0.5 ± 0.1
EWP 29	Low-Res	26	33.8 ± 2.1	0.3 ± 0.1
EWP 30	Low-Res	61	65.8 ± 3.0	0.9 ± 0.2
EWP 31	Low-Res	24	18.3 ± 1.5	0.2 ± 0.1
EWP 32	Low-Res	5548	5328 ± 22	141 ± 27
EWP 33	Low-Res	78	79.1 ± 2.9	1.4 ± 0.4
EWP 34	Low-Res	25	23.7 ± 1.8	0.4 ± 0.1

Table 8: The expected signal yields for the SUSY simplified model signals considered are shown for each search region bin in the $Hb\bar{b}$, $Zb\bar{b}$, and leptonic categories of the SP analysis. The bin names give a short-form description of the search region bin definition which are given in full in Table 2. The labels p_T^0, p_T^{75}, and p_T^{125} refer to bins defined by the requirement that $p_T^{\gamma\gamma}/m_{\gamma\gamma}$ is less than 0.6, between 0.6 and 1.0, and greater than 1.0, respectively. The labels m_{T2}^0 and m_{T2}^{30} refer to bins defined by the requirement that m_{T2} is less than and greater than 30 GeV, respectively. The labels HH and ZH refer to the signal models for higgsino-like chargino and neutralino production where the branching fractions of the decays $\widetilde{\chi}_1^0 \to H\widetilde{G}$ and $\widetilde{\chi}_1^0 \to Z\widetilde{G}$ are 100% and 0% , and 50% and 50%, respectively. For the above two scenarios, the mass of the chargino and next-to-lightest neutralino is 175 GeV, while the LSP mass is 45 GeV. The label WH (200,1) refers to the signal model for wino-like chargino and neutralino production, where the mass of the chargino and next-to-lightest neutralino is 200 GeV and the LSP mass is 1 GeV. The labels $\widetilde{b}$ (450,1) and $\widetilde{b}$ (450,300) refer to the signal models for bottom squark pair production where the bottom squark mass is 450 GeV and the LSP mass is 1 and 300 GeV, respectively.

Search region bin	Bin name	HH	ZH	WH (200,1)	$\widetilde{b}$ (450,1)	$\widetilde{b}$ (450,300)
SP 0	$Z_{\ell\ell}$	0.15 ± 0.02	1.2 ± 0.2	0.0 ± 0.0	0.07 ± 0.01	0.10 ± 0.01
SP 1	1μ p_T^0, m_{T2}^0	0.67 ± 0.11	0.22 ± 0.04	0.63 ± 0.07	0.69 ± 0.06	0.10 ± 0.01
SP 2	1μ p_T^0, m_{T2}^{30}	0.59 ± 0.10	0.23 ± 0.04	1.1 ± 0.1	0.88 ± 0.07	0.09 ± 0.01
SP 3	1μ p_T^{75}, m_{T2}^0	0.68 ± 0.09	0.22 ± 0.03	0.44 ± 0.04	0.40 ± 0.03	0.17 ± 0.01
SP 4	1μ p_T^{75}, m_{T2}^{30}	0.74 ± 0.09	0.27 ± 0.03	1.0 ± 0.1	0.45 ± 0.04	0.18 ± 0.01
SP 5	1μ p_T^{125}, m_{T2}^0	1.6 ± 0.3	0.51 ± 0.08	0.72 ± 0.14	0.24 ± 0.02	1.2 ± 0.1
SP 6	1μ p_T^{125}, m_{T2}^{30}	1.7 ± 0.3	0.58 ± 0.10	1.7 ± 0.3	0.32 ± 0.03	1.6 ± 0.1
SP 7	1e p_T^0, m_{T2}^0	0.43 ± 0.12	0.18 ± 0.03	0.41 ± 0.05	0.52 ± 0.04	0.06 ± 0.00
SP 8	1e p_T^0, m_{T2}^{30}	0.43 ± 0.11	0.19 ± 0.04	0.78 ± 0.12	0.52 ± 0.03	0.05 ± 0.00
SP 9	1e p_T^{75}, m_{T2}^0	0.45 ± 0.11	0.19 ± 0.02	0.30 ± 0.03	0.27 ± 0.02	0.12 ± 0.01
SP 10	1e p_T^{75}, m_{T2}^{30}	0.48 ± 0.09	0.22 ± 0.02	0.66 ± 0.07	0.29 ± 0.02	0.12 ± 0.01
SP 11	1e p_T^{125}, m_{T2}^0	1.3 ± 0.3	0.46 ± 0.09	0.60 ± 0.11	0.24 ± 0.02	0.87 ± 0.07
SP 12	1e p_T^{125}, m_{T2}^{30}	1.5 ± 0.3	0.57 ± 0.09	1.4 ± 0.3	0.28 ± 0.02	1.1 ± 0.1
SP 13	$Zb\bar{b}$ p_T^0, m_{T2}^0	1.3 ± 0.2	0.50 ± 0.08	0.09 ± 0.02	3.0 ± 0.2	0.29 ± 0.02
SP 14	$Zb\bar{b}$ p_T^{75}, m_{T2}^0	1.3 ± 0.1	0.52 ± 0.06	0.05 ± 0.01	1.7 ± 0.1	0.63 ± 0.04
SP 15	$Zb\bar{b}$ p_T^{125}, m_{T2}^0	2.9 ± 0.5	1.2 ± 0.2	0.11 ± 0.02	1.3 ± 0.1	5.1 ± 0.3
SP 16	$Zb\bar{b}$ p_T^0, m_{T2}^{30}	1.1 ± 0.2	0.49 ± 0.08	0.12 ± 0.02	2.5 ± 0.3	0.13 ± 0.01
SP 17	$Zb\bar{b}$ p_T^{75}, m_{T2}^{30}	1.1 ± 0.1	0.52 ± 0.07	0.13 ± 0.02	1.5 ± 0.1	0.31 ± 0.03
SP 18	$Zb\bar{b}$ p_T^{125}, m_{T2}^{30}	2.3 ± 0.4	1.3 ± 0.2	0.25 ± 0.05	1.1 ± 0.1	2.2 ± 0.2
SP 19	$Hb\bar{b}$ p_T^0, m_{T2}^0	2.9 ± 0.5	0.81 ± 0.14	0.03 ± 0.01	5.9 ± 0.4	1.4 ± 0.1
SP 20	$Hb\bar{b}$ p_T^{75}, m_{T2}^0	3.3 ± 0.3	0.91 ± 0.13	0.04 ± 0.01	3.4 ± 0.3	2.6 ± 0.2
SP 21	$Hb\bar{b}$ p_T^{125}, m_{T2}^0	9.6 ± 1.8	2.6 ± 0.5	0.06 ± 0.01	3.0 ± 0.2	22.7 ± 1.7
SP 22	$Hb\bar{b}$ p_T^0, m_{T2}^{30}	2.5 ± 0.4	0.71 ± 0.10	0.10 ± 0.01	4.7 ± 0.5	0.49 ± 0.05
SP 23	$Hb\bar{b}$ p_T^{75}, m_{T2}^{30}	2.9 ± 0.3	0.82 ± 0.10	0.11 ± 0.02	3.0 ± 0.3	0.86 ± 0.08
SP 24	$Hb\bar{b}$ p_T^{125}, m_{T2}^{30}	8.2 ± 1.6	2.4 ± 0.4	0.15 ± 0.04	2.8 ± 0.2	8.7 ± 0.7

Table 9: The expected signal yields for the SUSY simplified model signals considered are shown for each search region bin in the all-hadronic categories of the SP analysis. The bin names give a short-form description of the search region bin definition which are given in full in Table 3. The labels p_{T}^{0}, p_{T}^{75}, and p_{T}^{125} refer to bins defined by the requirement that $p_{\mathrm{T}}^{\gamma\gamma}/m_{\gamma\gamma}$ is less than 0.6, between 0.6 and 1.0, and greater than 1.0, respectively. The labels m_{T2}^{0} and m_{T2}^{30} refer to bins defined by the requirement that m_{T2} is less than and greater than 30 GeV, respectively. The labels for the different signal models are explained in detail in the caption of Table 8.

Search region bin	Bin name	HH	ZH	WH (200,1)	$\widetilde{\mathrm{b}}$ (450,1)	$\widetilde{\mathrm{b}}$ (450,300)
SP 25	0j, $\geq$0b, p_{T}^{0}	3.9 ± 0.6	2.9 ± 0.5	2.6 ± 0.3	2.7 ± 0.1	0.0 ± 0.0
SP 26	0j, $\geq$0b, p_{T}^{75}	2.4 ± 0.3	2.1 ± 0.2	1.8 ± 0.2	0.54 ± 0.02	0.0 ± 0.0
SP 27	0j, $\geq$0b, p_{T}^{125}	1.7 ± 0.2	2.7 ± 0.4	1.7 ± 0.2	0.15 ± 0.01	0.01 ± 0.00
SP 28	1–3j, 0b, p_{T}^{0}, m_{T2}^{0}	4.7 ± 0.8	2.7 ± 0.4	2.9 ± 0.3	4.2 ± 0.5	0.03 ± 0.00
SP 29	1–3j, 0b, p_{T}^{0}, m_{T2}^{30}	4.7 ± 0.5	2.6 ± 0.3	2.1 ± 0.2	1.6 ± 0.3	0.03 ± 0.01
SP 30	1–3j, 0b, p_{T}^{75}, m_{T2}^{0}	9.0 ± 1.5	5.1 ± 0.9	3.1 ± 0.6	0.73 ± 0.15	0.27 ± 0.05
SP 31	1–3j, 0b, p_{T}^{75}, m_{T2}^{30}	0.21 ± 0.04	0.10 ± 0.02	0.10 ± 0.01	0.34 ± 0.09	0.04 ± 0.01
SP 32	1–3j, 0b, p_{T}^{125}, m_{T2}^{0}	0.18 ± 0.02	0.10 ± 0.01	0.07 ± 0.01	0.15 ± 0.04	0.05 ± 0.01
SP 33	1–3j, 0b, p_{T}^{125}, m_{T2}^{30}	0.66 ± 0.14	0.35 ± 0.07	0.19 ± 0.04	0.14 ± 0.03	0.35 ± 0.07
SP 34	1–3j, 1b, p_{T}^{0}, m_{T2}^{0}	6.1 ± 0.9	2.2 ± 0.3	1.1 ± 0.1	7.1 ± 1.0	0.12 ± 0.02
SP 35	1–3j, 1b, p_{T}^{0}, m_{T2}^{30}	6.6 ± 0.6	2.4 ± 0.2	0.81 ± 0.06	3.4 ± 0.3	0.20 ± 0.02
SP 36	1–3j, 1b, p_{T}^{75}, m_{T2}^{0}	13.7 ± 2.1	5.1 ± 0.9	1.4 ± 0.2	2.2 ± 0.3	1.7 ± 0.2
SP 37	1–3j, 1b, p_{T}^{75}, m_{T2}^{30}	0.23 ± 0.03	0.09 ± 0.01	0.08 ± 0.01	0.82 ± 0.13	0.27 ± 0.04
SP 38	1–3j, 1b, p_{T}^{125}, m_{T2}^{0}	0.36 ± 0.04	0.13 ± 0.01	0.07 ± 0.00	0.39 ± 0.06	0.59 ± 0.08
SP 39	1–3j, 1b, p_{T}^{125}, m_{T2}^{30}	1.2 ± 0.2	0.47 ± 0.09	0.18 ± 0.03	0.37 ± 0.05	3.5 ± 0.5
SP 40	1–3j, $\geq$2b, p_{T}^{0}, m_{T2}^{0}	0.60 ± 0.09	0.21 ± 0.04	0.08 ± 0.01	1.9 ± 0.2	0.43 ± 0.05
SP 41	1–3j, $\geq$2b, p_{T}^{0}, m_{T2}^{30}	0.81 ± 0.07	0.27 ± 0.02	0.07 ± 0.01	1.2 ± 0.1	0.69 ± 0.07
SP 42	1–3j, $\geq$2b, p_{T}^{75}, m_{T2}^{0}	2.0 ± 0.4	0.67 ± 0.11	0.09 ± 0.03	0.98 ± 0.12	5.0 ± 0.6
SP 43	1–3j, $\geq$2b, p_{T}^{75}, m_{T2}^{30}	0.08 ± 0.01	0.03 ± 0.01	0.02 ± 0.01	0.38 ± 0.04	1.3 ± 0.1
SP 44	1–3j, $\geq$2b, p_{T}^{125}, m_{T2}^{0}	0.11 ± 0.03	0.04 ± 0.00	0.03 ± 0.00	0.28 ± 0.03	2.2 ± 0.2
SP 45	1–3j, $\geq$2b, p_{T}^{125}, m_{T2}^{30}	0.44 ± 0.10	0.16 ± 0.03	0.05 ± 0.03	0.37 ± 0.03	15.5 ± 1.3
SP 46	$\geq$4j, 0b, p_{T}^{0}, m_{T2}^{0}	3.9 ± 0.6	3.1 ± 0.5	6.6 ± 0.7	3.3 ± 0.8	0.01 ± 0.00
SP 47	$\geq$4j, 0b, p_{T}^{0}, m_{T2}^{30}	4.2 ± 0.5	3.4 ± 0.4	5.6 ± 0.5	1.2 ± 0.2	0.03 ± 0.01
SP 48	$\geq$4j, 0b, p_{T}^{75}, m_{T2}^{0}	7.5 ± 1.2	6.9 ± 1.2	8.0 ± 1.4	0.56 ± 0.11	0.13 ± 0.03
SP 49	$\geq$4j, 0b, p_{T}^{75}, m_{T2}^{30}	0.14 ± 0.02	0.10 ± 0.01	0.19 ± 0.02	0.52 ± 0.11	0.02 ± 0.00
SP 50	$\geq$4j, 0b, p_{T}^{125}, m_{T2}^{0}	0.16 ± 0.02	0.13 ± 0.02	0.19 ± 0.02	0.25 ± 0.05	0.02 ± 0.00
SP 51	$\geq$4j, 0b, p_{T}^{125}, m_{T2}^{30}	0.81 ± 0.18	0.50 ± 0.11	0.51 ± 0.11	0.27 ± 0.05	0.16 ± 0.03
SP 52	$\geq$4j, 1b, p_{T}^{0}, m_{T2}^{0}	5.0 ± 0.8	2.3 ± 0.3	2.5 ± 0.3	5.1 ± 0.9	0.08 ± 0.01
SP 53	$\geq$4j, 1b, p_{T}^{0}, m_{T2}^{30}	5.4 ± 0.6	2.5 ± 0.2	2.1 ± 0.2	2.3 ± 0.2	0.15 ± 0.02
SP 54	$\geq$4j, 1b, p_{T}^{75}, m_{T2}^{0}	11.4 ± 1.8	5.5 ± 0.9	3.5 ± 0.6	1.4 ± 0.2	1.1 ± 0.1
SP 55	$\geq$4j, 1b, p_{T}^{75}, m_{T2}^{30}	0.27 ± 0.03	0.14 ± 0.02	0.18 ± 0.02	1.2 ± 0.2	0.11 ± 0.01
SP 56	$\geq$4j, 1b, p_{T}^{125}, m_{T2}^{0}	0.33 ± 0.03	0.14 ± 0.01	0.17 ± 0.01	0.81 ± 0.13	0.15 ± 0.03
SP 57	$\geq$4j, 1b, p_{T}^{125}, m_{T2}^{30}	1.4 ± 0.3	0.65 ± 0.12	0.42 ± 0.09	0.76 ± 0.12	1.5 ± 0.2
SP 58	$\geq$4j, $\geq$2b, p_{T}^{0}, m_{T2}^{0}	0.42 ± 0.06	0.18 ± 0.03	0.16 ± 0.03	1.4 ± 0.1	0.18 ± 0.02
SP 59	$\geq$4j, $\geq$2b, p_{T}^{0}, m_{T2}^{30}	0.65 ± 0.07	0.26 ± 0.03	0.13 ± 0.02	0.86 ± 0.08	0.35 ± 0.03
SP 60	$\geq$4j, $\geq$2b, p_{T}^{75}, m_{T2}^{0}	1.6 ± 0.3	0.67 ± 0.11	0.24 ± 0.07	0.71 ± 0.08	2.4 ± 0.3
SP 61	$\geq$4j, $\geq$2b, p_{T}^{75}, m_{T2}^{30}	0.08 ± 0.02	0.03 ± 0.00	0.03 ± 0.01	0.73 ± 0.07	0.44 ± 0.04
SP 62	$\geq$4j, $\geq$2b, p_{T}^{125}, m_{T2}^{0}	0.14 ± 0.03	0.05 ± 0.02	0.03 ± 0.00	0.53 ± 0.06	0.82 ± 0.09
SP 63	$\geq$4j, $\geq$2b, p_{T}^{125}, m_{T2}^{30}	0.51 ± 0.11	0.20 ± 0.06	0.11 ± 0.03	0.57 ± 0.05	6.4 ± 0.6

Table 10: The expected signal yields for the SUSY simplified model signals considered are shown for each search region bin of the EWP analysis. The category that each search region bin belongs to is also indicated in the table. The search region bins definitions are summarized in Table 1. The labels for the different signal models are explained in detail in the caption of Table 8.

Search region bin	Category	HH	ZH	WH (200,1)	$\widetilde{b}$ (450,1)	$\widetilde{b}$ (450,300)
EWP 0	Two-Lepton	0.2 ± 0.01	1.6 ± 0.1	0.0 ± 0.000	0.2 ± 0.1	0.1 ± 0.03
EWP 1	Muon High-p_T	4.5 ± 0.2	1.5 ± 0.1	3.3 ± 0.2	4.4 ± 1.8	0.9 ± 0.4
EWP 2	Muon Low-p_T	1.6 ± 0.04	0.6 ± 0.02	1.7 ± 0.05	0.6 ± 0.2	1.8 ± 0.7
EWP 3	Electron High-p_T	4.0 ± 0.2	1.5 ± 0.1	2.7 ± 0.1	3.2 ± 1.3	0.8 ± 0.3
EWP 4	Electron Low-p_T	0.5 ± 0.01	0.2 ± 0.01	0.9 ± 0.04	0.1 ± 0.03	0.7 ± 0.3
EWP 5	Electron Low-p_T	0.3 ± 0.01	0.1 ± 0.01	0.2 ± 0.02	0.2 ± 0.1	0.2 ± 0.1
EWP 6	Electron Low-p_T	0.3 ± 0.01	0.2 ± 0.004	0.3 ± 0.02	0.1 ± 0.04	0.4 ± 0.2
EWP 7	$Hb\bar{b}$ High-p_T	11.9 ± 0.5	3.4 ± 0.2	0.2 ± 0.01	4.3 ± 4.3	4.7 ± 1.9
EWP 8	$Hb\bar{b}$ High-p_T	9.1 ± 0.6	2.5 ± 0.2	0.1 ± 0.005	30.1 ± 12.1	2.2 ± 0.8
EWP 9	$Hb\bar{b}$ Low-p_T	1.9 ± 0.2	0.6 ± 0.05	0.1 ± 0.003	0.8 ± 1.0	6.5 ± 2.8
EWP 10	$Hb\bar{b}$ Low-p_T	1.2 ± 0.1	0.4 ± 0.04	0.03 ± 0.002	3.7 ± 1.5	2.4 ± 1.0
EWP 11	$Zb\bar{b}$ High-p_T	3.2 ± 0.3	1.7 ± 0.2	0.3 ± 0.02	0.6 ± 0.6	1.9 ± 0.8
EWP 12	$Zb\bar{b}$ High-p_T	1.3 ± 0.2	0.6 ± 0.1	0.1 ± 0.01	4.8 ± 2.2	0.4 ± 0.2
EWP 13	$Zb\bar{b}$ High-p_T	2.5 ± 0.1	1.1 ± 0.1	0.1 ± 0.02	2.3 ± 2.2	1.0 ± 0.4
EWP 14	$Zb\bar{b}$ Low-p_T	1.7 ± 0.2	0.8 ± 0.1	0.2 ± 0.01	0.1 ± 0.1	3.7 ± 1.5
EWP 15	$Zb\bar{b}$ Low-p_T	0.6 ± 0.2	0.2 ± 0.04	0.02 ± 0.002	0.6 ± 0.3	0.8 ± 0.4
EWP 16	$Zb\bar{b}$ Low-p_T	1.0 ± 0.05	0.4 ± 0.02	0.04 ± 0.01	0.3 ± 0.3	1.5 ± 0.6
EWP 17	High-p_T	5.3 ± 1.6	5.5 ± 0.6	7.2 ± 0.5	0.3 ± 0.2	1.4 ± 0.7
EWP 18	High-p_T	1.8 ± 0.1	0.8 ± 0.05	0.5 ± 0.03	0.01 ± 0.1	0.3 ± 0.1
EWP 19	High-p_T	6.0 ± 1.4	4.0 ± 0.7	3.6 ± 0.2	0.6 ± 0.4	1.4 ± 0.6
EWP 20	High-p_T	42.1 ± 3.9	19.6 ± 1.8	9.1 ± 0.8	40.1 ± 15.8	6.1 ± 2.4
EWP 21	High-p_T	4.9 ± 0.2	2.3 ± 0.1	1.4 ± 0.1	0.03 ± 0.04	0.9 ± 0.4
EWP 22	High-p_T	7.3 ± 1.2	4.2 ± 0.6	3.0 ± 0.2	1.5 ± 1.4	1.3 ± 0.5
EWP 23	High-Res	1.1 ± 1.2	1.0 ± 0.4	3.0 ± 0.6	0.03 ± 0.02	2.2 ± 1.2
EWP 24	High-Res	1.5 ± 0.5	0.9 ± 0.2	1.1 ± 0.1	0.03 ± 0.01	1.4 ± 0.6
EWP 25	High-Res	0.6 ± 0.3	0.4 ± 0.1	0.6 ± 0.1	0.01 ± 0.2	0.6 ± 0.3
EWP 26	High-Res	13.7 ± 2.1	6.5 ± 1.0	4.4 ± 0.7	4.1 ± 1.7	10.4 ± 4.4
EWP 27	High-Res	0.5 ± 0.1	0.3 ± 0.04	0.2 ± 0.03	0.0 ± 0.000	0.4 ± 0.2
EWP 28	High-Res	0.8 ± 0.2	0.5 ± 0.1	0.6 ± 0.1	0.1 ± 0.2	0.9 ± 0.4
EWP 29	Low-Res	0.7 ± 0.7	0.7 ± 0.3	1.9 ± 0.5	0.02 ± 0.01	1.5 ± 0.8
EWP 30	Low-Res	1.0 ± 0.3	0.5 ± 0.1	0.7 ± 0.2	0.02 ± 0.01	1.0 ± 0.5
EWP 31	Low-Res	0.5 ± 0.4	0.3 ± 0.2	0.4 ± 0.1	0.01 ± 0.003	0.5 ± 0.3
EWP 32	Low-Res	8.4 ± 2.2	4.1 ± 1.0	3.0 ± 0.8	2.7 ± 1.3	7.1 ± 3.6
EWP 33	Low-Res	0.4 ± 0.1	0.2 ± 0.05	0.2 ± 0.04	0.002 ± 0.001	0.2 ± 0.1
EWP 34	Low-Res	0.6 ± 0.2	0.3 ± 0.1	0.4 ± 0.1	0.01 ± 0.01	0.6 ± 0.3

Acknowledgments

We congratulate our colleagues in the CERN accelerator departments for the excellent performance of the LHC and thank the technical and administrative staffs at CERN and at other CMS institutes for their contributions to the success of the CMS effort. In addition, we gratefully acknowledge the computing centers and personnel of the Worldwide LHC Computing Grid for delivering so effectively the computing infrastructure essential to our analyses. Finally, we acknowledge the enduring support for the construction and operation of the LHC and the CMS detector provided by the following funding agencies: BMBWF and FWF (Austria); FNRS and FWO (Belgium); CNPq, CAPES, FAPERJ, FAPERGS, and FAPESP (Brazil); MES (Bulgaria); CERN; CAS, MoST, and NSFC (China); COLCIENCIAS (Colombia); MSES and CSF (Croatia); RPF (Cyprus); SENESCYT (Ecuador); MoER, ERC IUT, PUT and ERDF (Estonia); Academy of Finland, MEC, and HIP (Finland); CEA and CNRS/IN2P3 (France); BMBF, DFG, and HGF (Germany); GSRT (Greece); NKFIA (Hungary); DAE and DST (India); IPM (Iran); SFI (Ireland); INFN (Italy); MSIP and NRF (Republic of Korea); MES (Latvia); LAS (Lithuania); MOE and UM (Malaysia); BUAP, CINVESTAV, CONACYT, LNS, SEP, and UASLP-FAI (Mexico); MOS (Montenegro); MBIE (New Zealand); PAEC (Pakistan); MSHE and NSC (Poland); FCT (Portugal); JINR (Dubna); MON, RosAtom, RAS, RFBR, and NRC KI (Russia); MESTD (Serbia); SEIDI, CPAN, PCTI, and FEDER (Spain); MOSTR (Sri Lanka); Swiss Funding Agencies (Switzerland); MST (Taipei); ThEPCenter, IPST, STAR, and NSTDA (Thailand); TUBITAK and TAEK (Turkey); NASU and SFFR (Ukraine); STFC (United Kingdom); DOE and NSF (USA).

Individuals have received support from the Marie-Curie program and the European Research Council and Horizon 2020 Grant, contract Nos. 675440, 752730, and 765710 (European Union); the Leventis Foundation; the A.P. Sloan Foundation; the Alexander von Humboldt Foundation; the Belgian Federal Science Policy Office; the Fonds pour la Formation à la Recherche dans l'Industrie et dans l'Agriculture (FRIA-Belgium); the Agentschap voor Innovatie door Wetenschap en Technologie (IWT-Belgium); the F.R.S.-FNRS and FWO (Belgium) under the "Excellence of Science – EOS" – be.h project n. 30820817; the Beijing Municipal Science & Technology Commission, No. Z181100004218003; the Ministry of Education, Youth and Sports (MEYS) of the Czech Republic; the Lendület ("Momentum") Program and the János Bolyai Research Scholarship of the Hungarian Academy of Sciences, the New National Excellence Program ÚNKP, the NKFIA research grants 123842, 123959, 124845, 124850, 125105, 128713, 128786, and 129058 (Hungary); the Council of Science and Industrial Research, India; the HOMING PLUS program of the Foundation for Polish Science, cofinanced from European Union, Regional Development Fund, the Mobility Plus program of the Ministry of Science and Higher Education, the National Science Center (Poland), contracts Harmonia 2014/14/M/ST2/00428, Opus 2014/13/B/ST2/02543, 2014/15/B/ST2/03998, and 2015/19/B/ST2/02861, Sonata-bis 2012/07/E/ST2/01406; the National Priorities Research Program by Qatar National Research Fund; the Ministry of Science and Education, grant no. 3.2989.2017 (Russia); the Programa Estatal de Fomento de la Investigación Científica y Técnica de Excelencia María de Maeztu, grant MDM-2015-0509 and the Programa Severo Ochoa del Principado de Asturias; the Thalis and Aristeia programs cofinanced by EU-ESF and the Greek NSRF; the Rachadapisek Sompot Fund for Postdoctoral Fellowship, Chulalongkorn University and the Chulalongkorn Academic into Its 2nd Century Project Advancement Project (Thailand); the Welch Foundation, contract C-1845; and the Weston Havens Foundation (USA).

References

[1] M. Monaco, M. Pierini, A. Romanino, and M. Spinrath, "Phenomenology of minimal unified tree level gauge mediation at the LHC", *JHEP* **07** (2013) 078, doi:10.1007/JHEP07(2013)078, arXiv:1302.1305.

[2] J. Duarte et al., "Squark-mediated Higgs+jets production at the LHC", (2017). arXiv:1703.06544.

[3] S. Dimopoulos and H. Georgi, "Softly broken supersymmetry and SU(5)", *Nucl. Phys. B* **193** (1981) 150, doi:10.1016/0550-3213(81)90522-8.

[4] S. Dimopoulos, M. Dine, S. Raby, and S. D. Thomas, "Experimental signatures of low-energy gauge mediated supersymmetry breaking", *Phys. Rev. Lett.* **76** (1996) 3494, doi:10.1103/PhysRevLett.76.3494, arXiv:hep-ph/9601367.

[5] K. T. Matchev and S. D. Thomas, "Higgs and Z boson signatures of supersymmetry", *Phys. Rev. D* **62** (2000) 077702, doi:10.1103/PhysRevD.62.077702, arXiv:hep-ph/9908482.

[6] ATLAS Collaboration, "Search for direct pair production of a chargino and a neutralino decaying to the 125 GeV Higgs boson in $\sqrt{s} = 8$ TeV pp collisions with the ATLAS detector", *Eur. Phys. J. C* **75** (2015) 208, doi:10.1140/epjc/s10052-015-3408-7, arXiv:1501.07110.

[7] CMS Collaboration, "Searches for electroweak neutralino and chargino production in channels with Higgs, Z, and W bosons in pp collisions at 8 TeV", *Phys. Rev. D* **90** (2014) 092007, doi:10.1103/PhysRevD.90.092007, arXiv:1409.3168.

[8] CMS Collaboration, "Search for supersymmetry with Higgs boson to diphoton decays using the razor variables at $\sqrt{s} = 13$ TeV", *Phys. Lett. B* **779** (2018) 166, doi:10.1016/j.physletb.2017.12.069, arXiv:1709.00384.

[9] ATLAS Collaboration, "Search for chargino and neutralino production in final states with a Higgs boson and missing transverse momentum at $\sqrt{s} = 13$ TeV with the ATLAS detector", (2018). arXiv:1812.09432. Submitted to: Phys. Rev. D.

[10] CMS Collaboration, "The CMS trigger system", *JINST* **12** (2017) P01020, doi:10.1088/1748-0221/12/01/P01020, arXiv:1609.02366.

[11] CMS Collaboration, "The CMS experiment at the CERN LHC", *JINST* **3** (2008) S08004, doi:10.1088/1748-0221/3/08/S08004.

[12] J. Alwall et al., "The automated computation of tree-level and next-to-leading order differential cross sections, and their matching to parton shower simulations", *JHEP* **07** (2014) 079, doi:10.1007/JHEP07(2014)079, arXiv:1405.0301.

[13] ATLAS and CMS Collaboration, "Combined measurement of the Higgs boson mass in pp collisions at $\sqrt{s} = 7$ and 8 TeV with the ATLAS and CMS experiments", *Phys. Rev. Lett.* **114** (2015) 191803, doi:10.1103/PhysRevLett.114.191803, arXiv:1503.07589.

[14] CMS Collaboration, "Measurements of properties of the Higgs boson decaying into the four-lepton final state in pp collisions at $\sqrt{s} = 13$ TeV", *JHEP* **11** (2017) 047, doi:10.1007/JHEP11(2017)047, arXiv:1706.09936.

[15] D. de Florian et al., "Handbook of LHC Higgs cross sections: 4. deciphering the nature of the Higgs sector", CERN Report CERN-2017-002-M, 2016. doi:10.23731/CYRM-2017-002, arXiv:1610.07922.

[16] R. Frederix and S. Frixione, "Merging meets matching in MC@NLO", *JHEP* **12** (2012) 061, doi:10.1007/JHEP12(2012)061, arXiv:1209.6215.

[17] J. Alwall et al., "Comparative study of various algorithms for the merging of parton showers and matrix elements in hadronic collisions", *Eur. Phys. J. C* **53** (2008) 473, doi:10.1140/epjc/s10052-007-0490-5, arXiv:0706.2569.

[18] T. Sjöstrand et al., "An Introduction to PYTHIA 8.2", *Comput. Phys. Commun.* **191** (2015) 159, doi:10.1016/j.cpc.2015.01.024, arXiv:1410.3012.

[19] P. Skands, S. Carrazza, and J. Rojo, "Tuning PYTHIA 8.1: the Monash 2013 tune", *Eur. Phys. J. C* **74** (2014) 3024, doi:10.1140/epjc/s10052-014-3024-y.

[20] CMS Collaboration, "Extraction and validation of a new set of CMS PYTHIA8 tunes from underlying-event measurements", (2019). arXiv:1903.12179. Submitted to EPJC.

[21] NNPDF Collaboration, "Parton distributions for the LHC Run II", *JHEP* **04** (2015) 040, doi:10.1007/JHEP04(2015)040, arXiv:1410.8849.

[22] NNPDF Collaboration, "Parton distributions from high-precision collider data", *Eur. Phys. J. C* **77** (2017) 663, doi:10.1140/epjc/s10052-017-5199-5, arXiv:1706.00428.

[23] GEANT4 Collaboration, "GEANT4—a simulation toolkit", *Nucl. Instrum. Meth. A* **506** (2003) 250, doi:10.1016/S0168-9002(03)01368-8.

[24] S. Abdullin et al., "The fast simulation of the CMS detector at LHC", *J. Phys. Conf. Ser.* **331** (2011) 032049, doi:10.1088/1742-6596/331/3/032049.

[25] A. Giammanco, "The fast simulation of the CMS experiment", *J. Phys. Conf. Ser.* **513** (2014) 022012, doi:10.1088/1742-6596/513/2/022012.

[26] CMS Collaboration, "Particle-flow reconstruction and global event description with the CMS detector", *JINST* **12** (2017) P10003, doi:10.1088/1748-0221/12/10/P10003, arXiv:1706.04965.

[27] M. Cacciari and G. P. Salam, "Pileup subtraction using jet areas", *Phys. Lett. B* **659** (2008) 119, doi:10.1016/j.physletb.2007.09.077, arXiv:0707.1378.

[28] M. Cacciari, G. P. Salam, and G. Soyez, "The anti-k_{T} jet clustering algorithm", *JHEP* **04** (2008) 063, doi:10.1088/1126-6708/2008/04/063, arXiv:0802.1189.

[29] M. Cacciari, G. P. Salam, and G. Soyez, "FastJet user manual", *Eur. Phys. J. C* **72** (2012) 1896, doi:10.1140/epjc/s10052-012-1896-2, arXiv:1111.6097.

[30] CMS Collaboration, "Jet energy scale and resolution in the CMS experiment in pp collisions at 8 TeV", *JINST* **12** (2017) P02014, doi:10.1088/1748-0221/12/02/P02014, arXiv:1607.03663.

[31] CMS Collaboration, "Identification of b-quark jets with the CMS experiment", *JINST* **8** (2013) P04013, doi:10.1088/1748-0221/8/04/P04013, arXiv:1211.4462.

[32] CMS Collaboration, "Missing transverse energy performance of the CMS detector", *JINST* **6** (2011) P09001, doi:10.1088/1748-0221/6/09/P09001, arXiv:1106.5048.

[33] C. Rogan, "Kinematical variables towards new dynamics at the LHC", (2010). arXiv:1006.2727.

[34] CMS Collaboration, "Inclusive search for supersymmetry using razor variables in pp collisions at $\sqrt{s} = 13$ TeV", *Phys. Rev. D* **95** (2017) 012003, doi:10.1103/PhysRevD.95.012003, arXiv:1609.07658.

[35] CMS Collaboration, "Search for new physics with the M_{T2} variable in all-jets final states produced in pp collisions at $\sqrt{s} = 13$ TeV", *JHEP* **10** (2016) 006, doi:10.1007/JHEP10(2016)006, arXiv:1603.04053.

[36] C. G. Lester and D. J. Summers, "Measuring masses of semi-invisibly decaying particles pair produced at hadron colliders", *Phys. Lett. B* **463** (1999) 99, doi:10.1016/S0370-2693(99)00945-4, arXiv:hep-ph/9906349.

[37] H. Akaike, "A new look at the statistical model identification", *IEEE Transactions on Automatic Control* **19-6** (1974) 716, doi:10.1109/TAC.1974.1100705.

[38] P. D. Dauncey, M. Kenzie, N. Wardle, and G. J. Davies, "Handling uncertainties in background shapes", *JINST* **10** (2015) P04015, doi:10.1088/1748-0221/10/04/P04015, arXiv:1408.6865.

[39] A. Kalogeropoulos and J. Alwall, "The SysCalc code: A tool to derive theoretical systematic uncertainties", (2018). arXiv:1801.08401.

[40] J. Butterworth et al., "PDF4LHC recommendations for LHC Run II", *J. Phys. G* **43** (2016) 023001, doi:10.1088/0954-3899/43/2/023001, arXiv:1510.03865.

[41] W. Beenakker, R. Höpker, M. Spira, and P. M. Zerwas, "Squark and gluino production at hadron colliders", *Nucl. Phys. B* **492** (1997) 51, doi:10.1016/S0550-3213(97)80027-2, arXiv:hep-ph/9610490.

[42] A. Kulesza and L. Motyka, "Threshold resummation for squark-antisquark and gluino-pair production at the LHC", *Phys. Rev. Lett.* **102** (2009) 111802, doi:10.1103/PhysRevLett.102.111802, arXiv:0807.2405.

[43] A. Kulesza and L. Motyka, "Soft gluon resummation for the production of gluino-gluino and squark-antisquark pairs at the LHC", *Phys. Rev. D* **80** (2009) 095004, doi:10.1103/PhysRevD.80.095004, arXiv:0905.4749.

[44] W. Beenakker et al., "Soft-gluon resummation for squark and gluino hadroproduction", *JHEP* **12** (2009) 041, doi:10.1088/1126-6708/2009/12/041, arXiv:0909.4418.

[45] W. Beenakker et al., "Squark and gluino hadroproduction", *Int. J. Mod. Phys. A* **26** (2011) 2637, doi:10.1142/S0217751X11053560, arXiv:1105.1110.

[46] C. Borschensky et al., "Squark and gluino production cross sections in pp collisions at $\sqrt{s} = 13$, 14, 33 and 100 TeV", *Eur. Phys. J. C* **74** (2014) 3174, doi:10.1140/epjc/s10052-014-3174-y, arXiv:1407.5066.

[47] W. Beenakker et al., "Production of charginos, neutralinos, and sleptons at hadron colliders", *Phys. Rev. Lett.* **83** (1999) 3780, doi:10.1103/PhysRevLett.83.3780, arXiv:hep-ph/9906298. [Erratum: doi:10.1103/PhysRevLett.100.029901].

[48] B. Fuks, M. Klasen, D. R. Lamprea, and M. Rothering, "Gaugino production in proton-proton collisions at a center-of-mass energy of 8 TeV", *JHEP* **10** (2012) 081, doi:10.1007/JHEP10(2012)081, arXiv:1207.2159.

[49] B. Fuks, M. Klasen, D. R. Lamprea, and M. Rothering, "Precision predictions for electroweak superpartner production at hadron colliders with RESUMMINO", *Eur. Phys. J. C* **73** (2013) 2480, doi:10.1140/epjc/s10052-013-2480-0, arXiv:1304.0790.

[50] P. Z. Skands and Others, "SUSY Les Houches accord: interfacing SUSY spectrum calculators, decay packages, and event generators", *JHEP* **07** (2004) 036, doi:10.1088/1126-6708/2004/07/036, arXiv:Hep-Ph/0311123.

[51] T. Junk, "Confidence level computation for combining searches with small statistics", *Nucl. Instrum. Meth. A* **434** (1999) 435, doi:10.1016/S0168-9002(99)00498-2, arXiv:hep-ex/9902006.

[52] A. L. Read, "Presentation of search results: The CL_s technique", *J. Phys. G* **28** (2002) 2693, doi:10.1088/0954-3899/28/10/313.

[53] ATLAS and CMS Collaborations, "Procedure for the LHC Higgs boson search combination in summer 2011", Technical Report ATL-PHYS-PUB-2011-011, CMS-NOTE-2011-005, 2011.

[54] G. Cowan, K. Cranmer, E. Gross, and O. Vitells, "Asymptotic formulae for likelihood-based tests of new physics", *Eur. Phys. J. C* **71** (2011) 1554, doi:10.1140/epjc/s10052-011-1554-0, arXiv:1007.1727. [Erratum: doi:10.1140/epjc/s10052-013-2501-z].

A Additional simplified model interpretations

While the EWP and SP analyses have greater expected sensitivity to electroweak and strong SUSY production, respectively, both analyses do have sensitivity to both production modes. In this appendix, we present limits obtained from the EWP and SP analyses for the simplified models that were not shown in Section 8.

The upper plot of Figure 6 shows the limits for sbottom pair production obtained using the EWP analysis, as a function of the bottom squark mass and the LSP mass.

For the wino-like chargino-neutralino production, the limits obtained using the SP analysis are shown in the lower plot of Fig. 6 as a function of the chargino mass and the LSP mass. Figure 7 shows the limits for the higgsino-like chargino-neutralino production simplified models obtained using the SP analysis as a function of the chargino mass for the case where the branching fraction of the $\widetilde{\chi}_1^0 \to \mathrm{H}\widetilde{\mathrm{G}}$ decay is 100% on the left, and for the case where the branching fraction of the $\widetilde{\chi}_1^0 \to \mathrm{H}\widetilde{\mathrm{G}}$ and $\widetilde{\chi}_1^0 \to \mathrm{Z}\widetilde{\mathrm{G}}$ decays are both 50% on the right.

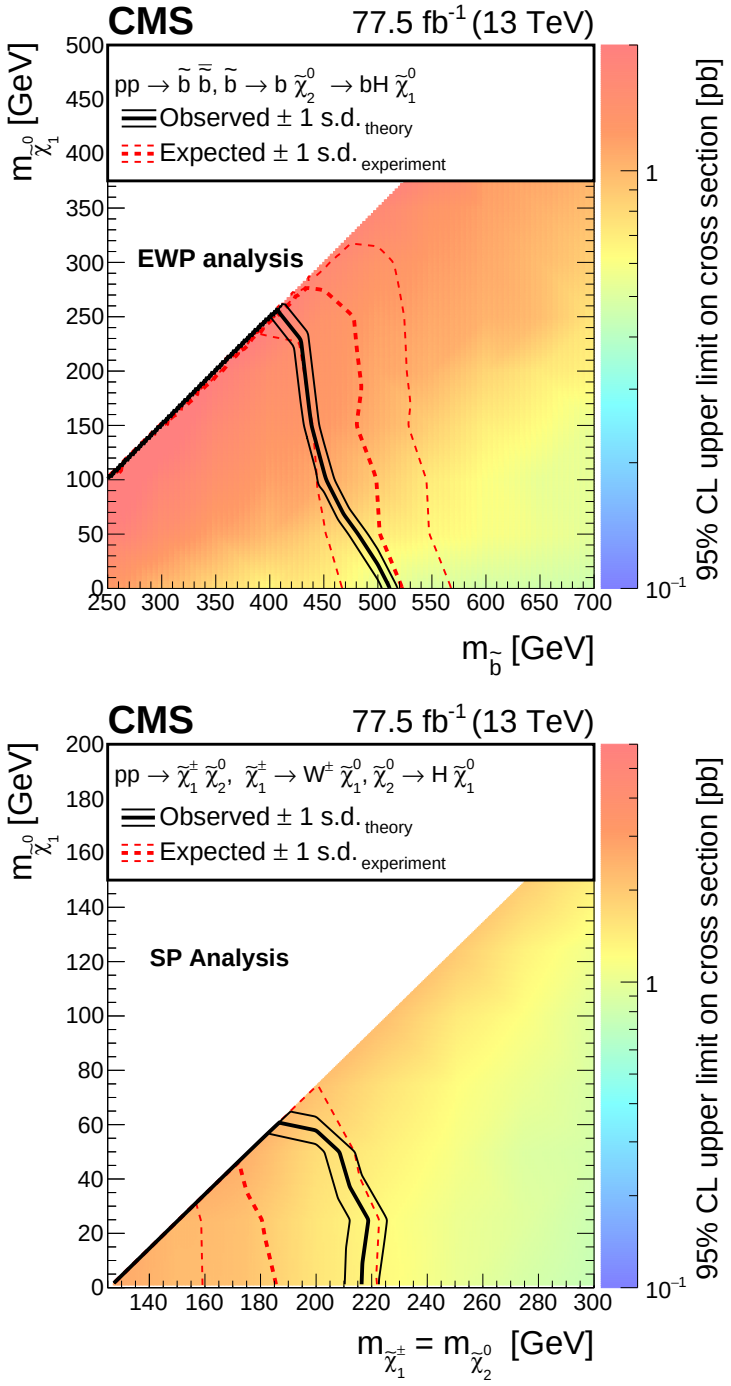

Figure 6: The observed 95% CL upper limits on the bottom squark pair production cross section for the EWP analysis (upper plot), and on the wino-like chargino-neutralino production cross section for the SP analysis (lower plot), are shown. The bold and light solid black contours represent the observed exclusion region and the ± 1 standard deviation (s.d.) band, including both experimental and theoretical uncertainties. The analogous red dotted contours represent the expected exclusion region and its ± 1 s.d. band.

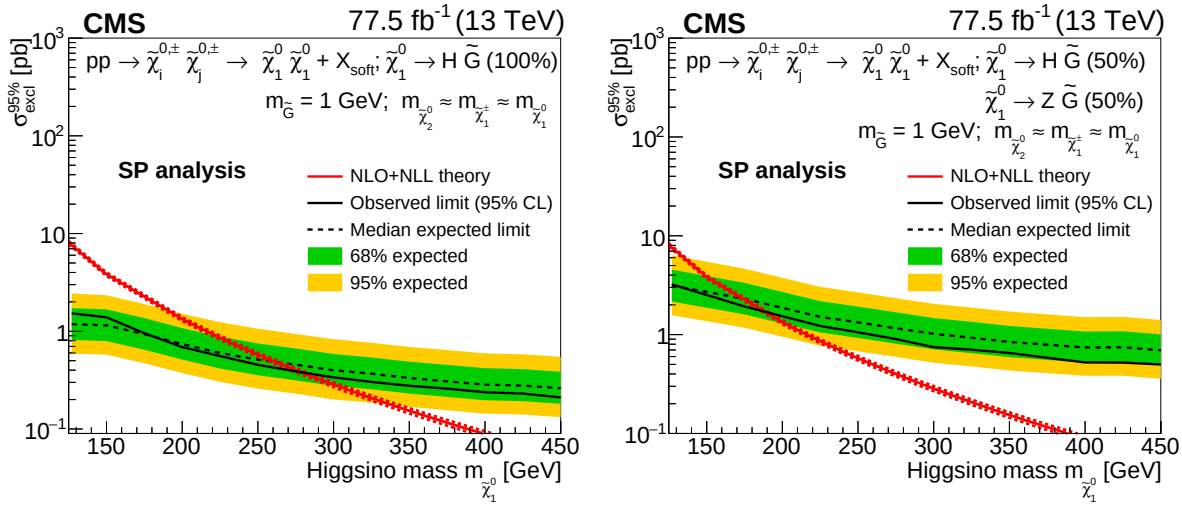

Figure 7: The observed 95% CL upper limits on the production cross section for higgsino-like chargino-neutralino production are shown for the SP analysis. The charginos and neutralinos undergo several cascade decays producing either Higgs bosons (left plot), or a Higgs boson and a Z boson (right plot). We present limits in the scenario where the branching fraction of $\widetilde{\chi}_1^0 \to \mathrm{H}\widetilde{\mathrm{G}}$ decay is 100% (left plot), and where the $\widetilde{\chi}_1^0 \to \mathrm{H}\widetilde{\mathrm{G}}$ and $\widetilde{\chi}_1^0 \to \mathrm{Z}\widetilde{\mathrm{G}}$ decays are each 50% (right plot). The dotted and solid black curves represent the expected and observed exclusion region, and the green dark and yellow light bands represent the ± 1 and ± 2 standard deviation regions, respectively. The red solid and dotted lines show the theoretical production cross section and its uncertainty band.

B The CMS Collaboration

Yerevan Physics Institute, Yerevan, Armenia
A.M. Sirunyan[†], A. Tumasyan

Institut für Hochenergiephysik, Wien, Austria
W. Adam, F. Ambrogi, T. Bergauer, J. Brandstetter, M. Dragicevic, J. Erö, A. Escalante Del Valle, M. Flechl, R. Frühwirth[1], M. Jeitler[1], N. Krammer, I. Krätschmer, D. Liko, T. Madlener, I. Mikulec, N. Rad, J. Schieck[1], R. Schöfbeck, M. Spanring, D. Spitzbart, W. Waltenberger, C.-E. Wulz[1], M. Zarucki

Institute for Nuclear Problems, Minsk, Belarus
V. Drugakov, V. Mossolov, J. Suarez Gonzalez

Universiteit Antwerpen, Antwerpen, Belgium
M.R. Darwish, E.A. De Wolf, D. Di Croce, X. Janssen, A. Lelek, M. Pieters, H. Rejeb Sfar, H. Van Haevermaet, P. Van Mechelen, S. Van Putte, N. Van Remortel

Vrije Universiteit Brussel, Brussel, Belgium
F. Blekman, E.S. Bols, S.S. Chhibra, J. D'Hondt, J. De Clercq, D. Lontkovskyi, S. Lowette, I. Marchesini, S. Moortgat, Q. Python, K. Skovpen, S. Tavernier, W. Van Doninck, P. Van Mulders

Université Libre de Bruxelles, Bruxelles, Belgium
D. Beghin, B. Bilin, H. Brun, B. Clerbaux, G. De Lentdecker, H. Delannoy, B. Dorney, L. Favart, A. Grebenyuk, A.K. Kalsi, A. Popov, N. Postiau, E. Starling, L. Thomas, C. Vander Velde, P. Vanlaer, D. Vannerom

Ghent University, Ghent, Belgium
T. Cornelis, D. Dobur, I. Khvastunov[2], M. Niedziela, C. Roskas, D. Trocino, M. Tytgat, W. Verbeke, B. Vermassen, M. Vit, N. Zaganidis

Université Catholique de Louvain, Louvain-la-Neuve, Belgium
O. Bondu, G. Bruno, C. Caputo, P. David, C. Delaere, M. Delcourt, A. Giammanco, V. Lemaitre, A. Magitteri, J. Prisciandaro, A. Saggio, M. Vidal Marono, P. Vischia, J. Zobec

Centro Brasileiro de Pesquisas Fisicas, Rio de Janeiro, Brazil
F.L. Alves, G.A. Alves, G. Correia Silva, C. Hensel, A. Moraes, P. Rebello Teles

Universidade do Estado do Rio de Janeiro, Rio de Janeiro, Brazil
E. Belchior Batista Das Chagas, W. Carvalho, J. Chinellato[3], E. Coelho, E.M. Da Costa, G.G. Da Silveira[4], D. De Jesus Damiao, C. De Oliveira Martins, S. Fonseca De Souza, L.M. Huertas Guativa, H. Malbouisson, J. Martins[5], D. Matos Figueiredo, M. Medina Jaime[6], M. Melo De Almeida, C. Mora Herrera, L. Mundim, H. Nogima, W.L. Prado Da Silva, L.J. Sanchez Rosas, A. Santoro, A. Sznajder, M. Thiel, E.J. Tonelli Manganote[3], F. Torres Da Silva De Araujo, A. Vilela Pereira

Universidade Estadual Paulista [a], Universidade Federal do ABC [b], São Paulo, Brazil
C.A. Bernardes[a], L. Calligaris[a], T.R. Fernandez Perez Tomei[a], E.M. Gregores[b], D.S. Lemos, P.G. Mercadante[b], S.F. Novaes[a], SandraS. Padula[a]

Institute for Nuclear Research and Nuclear Energy, Bulgarian Academy of Sciences, Sofia, Bulgaria
A. Aleksandrov, G. Antchev, R. Hadjiiska, P. Iaydjiev, M. Misheva, M. Rodozov, M. Shopova, G. Sultanov

University of Sofia, Sofia, Bulgaria
M. Bonchev, A. Dimitrov, T. Ivanov, L. Litov, B. Pavlov, P. Petkov

Beihang University, Beijing, China
W. Fang[7], X. Gao[7], L. Yuan

Institute of High Energy Physics, Beijing, China
M. Ahmad, G.M. Chen, H.S. Chen, M. Chen, C.H. Jiang, D. Leggat, H. Liao, Z. Liu, S.M. Shaheen[8], A. Spiezia, J. Tao, E. Yazgan, H. Zhang, S. Zhang[8], J. Zhao

State Key Laboratory of Nuclear Physics and Technology, Peking University, Beijing, China
A. Agapitos, Y. Ban, G. Chen, A. Levin, J. Li, L. Li, Q. Li, Y. Mao, S.J. Qian, D. Wang, Q. Wang

Tsinghua University, Beijing, China
Z. Hu, Y. Wang

Zhejiang University - Department of Physics
M. Xiao

Universidad de Los Andes, Bogota, Colombia
C. Avila, A. Cabrera, C. Florez, C.F. González Hernández, M.A. Segura Delgado

Universidad de Antioquia, Medellin, Colombia
J. Mejia Guisao, J.D. Ruiz Alvarez, C.A. Salazar González, N. Vanegas Arbelaez

University of Split, Faculty of Electrical Engineering, Mechanical Engineering and Naval Architecture, Split, Croatia
D. Giljanović, N. Godinovic, D. Lelas, I. Puljak, T. Sculac

University of Split, Faculty of Science, Split, Croatia
Z. Antunovic, M. Kovac

Institute Rudjer Boskovic, Zagreb, Croatia
V. Brigljevic, S. Ceci, D. Ferencek, K. Kadija, B. Mesic, M. Roguljic, A. Starodumov[9], T. Susa

University of Cyprus, Nicosia, Cyprus
M.W. Ather, A. Attikis, E. Erodotou, A. Ioannou, M. Kolosova, S. Konstantinou, G. Mavromanolakis, J. Mousa, C. Nicolaou, F. Ptochos, P.A. Razis, H. Rykaczewski, D. Tsiakkouri

Charles University, Prague, Czech Republic
M. Finger[10], M. Finger Jr.[10], A. Kveton, J. Tomsa

Escuela Politecnica Nacional, Quito, Ecuador
E. Ayala

Universidad San Francisco de Quito, Quito, Ecuador
E. Carrera Jarrin

Academy of Scientific Research and Technology of the Arab Republic of Egypt, Egyptian Network of High Energy Physics, Cairo, Egypt
S. Abu Zeid[11], S. Khalil[12]

National Institute of Chemical Physics and Biophysics, Tallinn, Estonia
S. Bhowmik, A. Carvalho Antunes De Oliveira, R.K. Dewanjee, K. Ehataht, M. Kadastik, M. Raidal, C. Veelken

Department of Physics, University of Helsinki, Helsinki, Finland
P. Eerola, L. Forthomme, H. Kirschenmann, K. Osterberg, M. Voutilainen

Helsinki Institute of Physics, Helsinki, Finland
F. Garcia, J. Havukainen, J.K. Heikkilä, T. Järvinen, V. Karimäki, M.S. Kim, R. Kinnunen, T. Lampén, K. Lassila-Perini, S. Laurila, S. Lehti, T. Lindén, P. Luukka, T. Mäenpää, H. Siikonen, E. Tuominen, J. Tuominiemi

Lappeenranta University of Technology, Lappeenranta, Finland
T. Tuuva

IRFU, CEA, Université Paris-Saclay, Gif-sur-Yvette, France
M. Besancon, F. Couderc, M. Dejardin, D. Denegri, B. Fabbro, J.L. Faure, F. Ferri, S. Ganjour, A. Givernaud, P. Gras, G. Hamel de Monchenault, P. Jarry, C. Leloup, E. Locci, J. Malcles, J. Rander, A. Rosowsky, M.Ö. Sahin, A. Savoy-Navarro[13], M. Titov

Laboratoire Leprince-Ringuet, Ecole polytechnique, CNRS/IN2P3, Université Paris-Saclay, Palaiseau, France
S. Ahuja, C. Amendola, F. Beaudette, P. Busson, C. Charlot, B. Diab, G. Falmagne, R. Granier de Cassagnac, I. Kucher, A. Lobanov, C. Martin Perez, M. Nguyen, C. Ochando, P. Paganini, J. Rembser, R. Salerno, J.B. Sauvan, Y. Sirois, A. Zabi, A. Zghiche

Université de Strasbourg, CNRS, IPHC UMR 7178, Strasbourg, France
J.-L. Agram[14], J. Andrea, D. Bloch, G. Bourgatte, J.-M. Brom, E.C. Chabert, C. Collard, E. Conte[14], J.-C. Fontaine[14], D. Gelé, U. Goerlach, M. Jansová, A.-C. Le Bihan, N. Tonon, P. Van Hove

Centre de Calcul de l'Institut National de Physique Nucleaire et de Physique des Particules, CNRS/IN2P3, Villeurbanne, France
S. Gadrat

Université de Lyon, Université Claude Bernard Lyon 1, CNRS-IN2P3, Institut de Physique Nucléaire de Lyon, Villeurbanne, France
S. Beauceron, C. Bernet, G. Boudoul, C. Camen, A. Carle, N. Chanon, R. Chierici, D. Contardo, P. Depasse, H. El Mamouni, J. Fay, S. Gascon, M. Gouzevitch, B. Ille, Sa. Jain, F. Lagarde, I.B. Laktineh, H. Lattaud, A. Lesauvage, M. Lethuillier, L. Mirabito, S. Perries, V. Sordini, L. Torterotot, G. Touquet, M. Vander Donckt, S. Viret

Georgian Technical University, Tbilisi, Georgia
A. Khvedelidze[10]

Tbilisi State University, Tbilisi, Georgia
Z. Tsamalaidze[10]

RWTH Aachen University, I. Physikalisches Institut, Aachen, Germany
C. Autermann, L. Feld, M.K. Kiesel, K. Klein, M. Lipinski, D. Meuser, A. Pauls, M. Preuten, M.P. Rauch, C. Schomakers, J. Schulz, M. Teroerde, B. Wittmer

RWTH Aachen University, III. Physikalisches Institut A, Aachen, Germany
A. Albert, M. Erdmann, B. Fischer, S. Ghosh, T. Hebbeker, K. Hoepfner, H. Keller, L. Mastrolorenzo, M. Merschmeyer, A. Meyer, P. Millet, G. Mocellin, S. Mondal, S. Mukherjee, D. Noll, A. Novak, T. Pook, A. Pozdnyakov, T. Quast, M. Radziej, Y. Rath, H. Reithler, J. Roemer, A. Schmidt, S.C. Schuler, A. Sharma, S. Wiedenbeck, S. Zaleski

RWTH Aachen University, III. Physikalisches Institut B, Aachen, Germany
G. Flügge, W. Haj Ahmad[15], O. Hlushchenko, T. Kress, T. Müller, A. Nehrkorn, A. Nowack, C. Pistone, O. Pooth, D. Roy, H. Sert, A. Stahl[16]

Deutsches Elektronen-Synchrotron, Hamburg, Germany
M. Aldaya Martin, P. Asmuss, I. Babounikau, H. Bakhshiansohi, K. Beernaert, O. Behnke, A. Bermúdez Martínez, D. Bertsche, A.A. Bin Anuar, K. Borras[17], V. Botta, A. Campbell, A. Cardini, P. Connor, S. Consuegra Rodríguez, C. Contreras-Campana, V. Danilov, A. De Wit, M.M. Defranchis, C. Diez Pardos, D. Domínguez Damiani, G. Eckerlin, D. Eckstein, T. Eichhorn, A. Elwood, E. Eren, E. Gallo[18], A. Geiser, A. Grohsjean, M. Guthoff, M. Haranko, A. Harb, A. Jafari, N.Z. Jomhari, H. Jung, A. Kasem[17], M. Kasemann, H. Kaveh, J. Keaveney, C. Kleinwort, J. Knolle, D. Krücker, W. Lange, T. Lenz, J. Leonard, J. Lidrych, K. Lipka, W. Lohmann[19], R. Mankel, I.-A. Melzer-Pellmann, A.B. Meyer, M. Meyer, M. Missiroli, G. Mittag, J. Mnich, A. Mussgiller, V. Myronenko, D. Pérez Adán, S.K. Pflitsch, D. Pitzl, A. Raspereza, A. Saibel, M. Savitskyi, V. Scheurer, P. Schütze, C. Schwanenberger, R. Shevchenko, A. Singh, H. Tholen, O. Turkot, A. Vagnerini, M. Van De Klundert, R. Walsh, Y. Wen, K. Wichmann, C. Wissing, O. Zenaiev, R. Zlebcik

University of Hamburg, Hamburg, Germany
R. Aggleton, S. Bein, L. Benato, A. Benecke, V. Blobel, T. Dreyer, A. Ebrahimi, F. Feindt, A. Fröhlich, C. Garbers, E. Garutti, D. Gonzalez, P. Gunnellini, J. Haller, A. Hinzmann, A. Karavdina, G. Kasieczka, R. Klanner, R. Kogler, N. Kovalchuk, S. Kurz, V. Kutzner, J. Lange, T. Lange, A. Malara, J. Multhaup, C.E.N. Niemeyer, A. Perieanu, A. Reimers, O. Rieger, C. Scharf, P. Schleper, S. Schumann, J. Schwandt, J. Sonneveld, H. Stadie, G. Steinbrück, F.M. Stober, M. Stöver, B. Vormwald, I. Zoi

Karlsruher Institut fuer Technologie, Karlsruhe, Germany
M. Akbiyik, C. Barth, M. Baselga, S. Baur, T. Berger, E. Butz, R. Caspart, T. Chwalek, W. De Boer, A. Dierlamm, K. El Morabit, N. Faltermann, M. Giffels, P. Goldenzweig, A. Gottmann, M.A. Harrendorf, F. Hartmann[16], U. Husemann, S. Kudella, S. Mitra, M.U. Mozer, D. Müller, Th. Müller, M. Musich, A. Nürnberg, G. Quast, K. Rabbertz, M. Schröder, I. Shvetsov, H.J. Simonis, R. Ulrich, M. Wassmer, M. Weber, C. Wöhrmann, R. Wolf

Institute of Nuclear and Particle Physics (INPP), NCSR Demokritos, Aghia Paraskevi, Greece
G. Anagnostou, P. Asenov, G. Daskalakis, T. Geralis, A. Kyriakis, D. Loukas, G. Paspalaki

National and Kapodistrian University of Athens, Athens, Greece
M. Diamantopoulou, G. Karathanasis, P. Kontaxakis, A. Manousakis-katsikakis, A. Panagiotou, I. Papavergou, N. Saoulidou, A. Stakia, K. Theofilatos, K. Vellidis, E. Vourliotis

National Technical University of Athens, Athens, Greece
G. Bakas, K. Kousouris, I. Papakrivopoulos, G. Tsipolitis

University of Ioánnina, Ioánnina, Greece
I. Evangelou, C. Foudas, P. Gianneios, P. Katsoulis, P. Kokkas, S. Mallios, K. Manitara, N. Manthos, I. Papadopoulos, J. Strologas, F.A. Triantis, D. Tsitsonis

MTA-ELTE Lendület CMS Particle and Nuclear Physics Group, Eötvös Loránd University, Budapest, Hungary
M. Bartók[20], R. Chudasama, M. Csanad, P. Major, K. Mandal, A. Mehta, M.I. Nagy, G. Pasztor, O. Surányi, G.I. Veres

Wigner Research Centre for Physics, Budapest, Hungary
G. Bencze, C. Hajdu, D. Horvath[21], F. Sikler, T.. Vámi, V. Veszpremi, G. Vesztergombi†

Institute of Nuclear Research ATOMKI, Debrecen, Hungary
N. Beni, S. Czellar, J. Karancsi[20], A. Makovec, J. Molnar, Z. Szillasi

Institute of Physics, University of Debrecen, Debrecen, Hungary
P. Raics, D. Teyssier, Z.L. Trocsanyi, B. Ujvari

Eszterhazy Karoly University, Karoly Robert Campus, Gyongyos, Hungary
T. Csorgo, W.J. Metzger, F. Nemes, T. Novak

Indian Institute of Science (IISc), Bangalore, India
S. Choudhury, J.R. Komaragiri, P.C. Tiwari

National Institute of Science Education and Research, HBNI, Bhubaneswar, India
S. Bahinipati[23], C. Kar, G. Kole, P. Mal, V.K. Muraleedharan Nair Bindhu, A. Nayak[24], D.K. Sahoo[23], S.K. Swain

Panjab University, Chandigarh, India
S. Bansal, S.B. Beri, V. Bhatnagar, S. Chauhan, R. Chawla, N. Dhingra, R. Gupta, A. Kaur, M. Kaur, S. Kaur, P. Kumari, M. Lohan, M. Meena, K. Sandeep, S. Sharma, J.B. Singh, A.K. Virdi

University of Delhi, Delhi, India
A. Bhardwaj, B.C. Choudhary, R.B. Garg, M. Gola, S. Keshri, Ashok Kumar, S. Malhotra, M. Naimuddin, P. Priyanka, K. Ranjan, Aashaq Shah, R. Sharma

Saha Institute of Nuclear Physics, HBNI, Kolkata, India
R. Bhardwaj[25], M. Bharti[25], R. Bhattacharya, S. Bhattacharya, U. Bhawandeep[25], D. Bhowmik, S. Dutta, S. Ghosh, M. Maity[26], K. Mondal, S. Nandan, A. Purohit, P.K. Rout, G. Saha, S. Sarkar, T. Sarkar[26], M. Sharan, B. Singh[25], S. Thakur[25]

Indian Institute of Technology Madras, Madras, India
P.K. Behera, P. Kalbhor, A. Muhammad, P.R. Pujahari, A. Sharma, A.K. Sikdar

Bhabha Atomic Research Centre, Mumbai, India
D. Dutta, V. Jha, V. Kumar, D.K. Mishra, P.K. Netrakanti, L.M. Pant, P. Shukla

Tata Institute of Fundamental Research-A, Mumbai, India
T. Aziz, M.A. Bhat, S. Dugad, G.B. Mohanty, N. Sur, RavindraKumar Verma

Tata Institute of Fundamental Research-B, Mumbai, India
S. Banerjee, S. Bhattacharya, S. Chatterjee, P. Das, M. Guchait, S. Karmakar, S. Kumar, G. Majumder, K. Mazumdar, N. Sahoo, S. Sawant

Indian Institute of Science Education and Research (IISER), Pune, India
S. Chauhan, S. Dube, V. Hegde, B. Kansal, A. Kapoor, K. Kothekar, S. Pandey, A. Rane, A. Rastogi, S. Sharma

Institute for Research in Fundamental Sciences (IPM), Tehran, Iran
S. Chenarani[27], E. Eskandari Tadavani, S.M. Etesami[27], M. Khakzad, M. Mohammadi Najafabadi, M. Naseri, F. Rezaei Hosseinabadi

University College Dublin, Dublin, Ireland
M. Felcini, M. Grunewald

INFN Sezione di Bari [a], Università di Bari [b], Politecnico di Bari [c], Bari, Italy
M. Abbrescia[a,b], R. Aly[a,b,28], C. Calabria[a,b], A. Colaleo[a], D. Creanza[a,c], L. Cristella[a,b], N. De Filippis[a,c], M. De Palma[a,b], A. Di Florio[a,b], L. Fiore[a], A. Gelmi[a,b], G. Iaselli[a,c], M. Ince[a,b], S. Lezki[a,b], G. Maggi[a,c], M. Maggi[a], G. Miniello[a,b], S. My[a,b], S. Nuzzo[a,b], A. Pompili[a,b], G. Pugliese[a,c], R. Radogna[a], A. Ranieri[a], G. Selvaggi[a,b], L. Silvestris[a], R. Venditti[a], P. Verwilligen[a]

INFN Sezione di Bologna [a], Università di Bologna [b], Bologna, Italy
G. Abbiendi[a], C. Battilana[a,b], D. Bonacorsi[a,b], L. Borgonovi[a,b], S. Braibant-Giacomelli[a,b], R. Campanini[a,b], P. Capiluppi[a,b], A. Castro[a,b], F.R. Cavallo[a], C. Ciocca[a], G. Codispoti[a,b], M. Cuffiani[a,b], G.M. Dallavalle[a], F. Fabbri[a], A. Fanfani[a,b], E. Fontanesi[a,b], P. Giacomelli[a], C. Grandi[a], L. Guiducci[a,b], F. Iemmi[a,b], S. Lo Meo[a,29], S. Marcellini[a], G. Masetti[a], F.L. Navarria[a,b], A. Perrotta[a], F. Primavera[a,b], A.M. Rossi[a,b], T. Rovelli[a,b], G.P. Siroli[a,b], N. Tosi[a]

INFN Sezione di Catania [a], Università di Catania [b], Catania, Italy
S. Albergo[a,b,30], S. Costa[a,b], A. Di Mattia[a], R. Potenza[a,b], A. Tricomi[a,b,30], C. Tuve[a,b]

INFN Sezione di Firenze [a], Università di Firenze [b], Firenze, Italy
G. Barbagli[a], A. Cassese, R. Ceccarelli, K. Chatterjee[a,b], V. Ciulli[a,b], C. Civinini[a], R. D'Alessandro[a,b], E. Focardi[a,b], G. Latino[a,b], P. Lenzi[a,b], M. Meschini[a], S. Paoletti[a], G. Sguazzoni[a], L. Viliani[a]

INFN Laboratori Nazionali di Frascati, Frascati, Italy
L. Benussi, S. Bianco, D. Piccolo

INFN Sezione di Genova [a], Università di Genova [b], Genova, Italy
M. Bozzo[a,b], F. Ferro[a], R. Mulargia[a,b], E. Robutti[a], S. Tosi[a,b]

INFN Sezione di Milano-Bicocca [a], Università di Milano-Bicocca [b], Milano, Italy
A. Benaglia[a], A. Beschi[a,b], F. Brivio[a,b], V. Ciriolo[a,b,16], S. Di Guida[a,b,16], M.E. Dinardo[a,b], P. Dini[a], S. Gennai[a], A. Ghezzi[a,b], P. Govoni[a,b], L. Guzzi[a,b], M. Malberti[a], S. Malvezzi[a], D. Menasce[a], F. Monti[a,b], L. Moroni[a], M. Paganoni[a,b], D. Pedrini[a], S. Ragazzi[a,b], T. Tabarelli de Fatis[a,b], D. Zuolo[a,b]

INFN Sezione di Napoli [a], Università di Napoli 'Federico II' [b], Napoli, Italy, Università della Basilicata [c], Potenza, Italy, Università G. Marconi [d], Roma, Italy
S. Buontempo[a], N. Cavallo[a,c], A. De Iorio[a,b], A. Di Crescenzo[a,b], F. Fabozzi[a,c], F. Fienga[a], G. Galati[a], A.O.M. Iorio[a,b], L. Lista[a,b], S. Meola[a,d,16], P. Paolucci[a,16], B. Rossi[a], C. Sciacca[a,b], E. Voevodina[a,b]

INFN Sezione di Padova [a], Università di Padova [b], Padova, Italy, Università di Trento [c], Trento, Italy
P. Azzi[a], N. Bacchetta[a], D. Bisello[a,b], A. Boletti[a,b], A. Bragagnolo[a,b], R. Carlin[a,b], P. Checchia[a], P. De Castro Manzano[a], T. Dorigo[a], U. Dosselli[a], F. Gasparini[a,b], U. Gasparini[a,b], A. Gozzelino[a], S.Y. Hoh[a,b], P. Lujan[a], M. Margoni[a,b], A.T. Meneguzzo[a,b], J. Pazzini[a,b], M. Presilla[b], P. Ronchese[a,b], R. Rossin[a,b], F. Simonetto[a,b], A. Tiko[a], M. Tosi[a,b], M. Zanetti[a,b], P. Zotto[a,b], G. Zumerle[a,b]

INFN Sezione di Pavia [a], Università di Pavia [b], Pavia, Italy
A. Braghieri[a], D. Fiorina[a,b], P. Montagna[a,b], S.P. Ratti[a,b], V. Re[a], M. Ressegotti[a,b], C. Riccardi[a,b], P. Salvini[a], I. Vai[a], P. Vitulo[a,b]

INFN Sezione di Perugia [a], Università di Perugia [b], Perugia, Italy
M. Biasini[a,b], G.M. Bilei[a], D. Ciangottini[a,b], L. Fanò[a,b], P. Lariccia[a,b], R. Leonardi[a,b], G. Mantovani[a,b], V. Mariani[a,b], M. Menichelli[a], A. Rossi[a,b], A. Santocchia[a,b], D. Spiga[a]

INFN Sezione di Pisa [a], Università di Pisa [b], Scuola Normale Superiore di Pisa [c], Pisa, Italy
K. Androsov[a], P. Azzurri[a], G. Bagliesi[a], V. Bertacchi[a,c], L. Bianchini[a], T. Boccali[a], R. Castaldi[a], M.A. Ciocci[a,b], R. Dell'Orso[a], G. Fedi[a], L. Giannini[a,c], A. Giassi[a], M.T. Grippo[a], F. Ligabue[a,c], E. Manca[a,c], G. Mandorli[a,c], A. Messineo[a,b], F. Palla[a], A. Rizzi[a,b], G. Rolandi[31],

S. Roy Chowdhury, A. Scribano[a], P. Spagnolo[a], R. Tenchini[a], G. Tonelli[a,b], N. Turini, A. Venturi[a], P.G. Verdini[a]

INFN Sezione di Roma [a], Sapienza Università di Roma [b], Rome, Italy
F. Cavallari[a], M. Cipriani[a,b], D. Del Re[a,b], E. Di Marco[a,b], M. Diemoz[a], E. Longo[a,b], B. Marzocchi[a,b], P. Meridiani[a], G. Organtini[a,b], F. Pandolfi[a], R. Paramatti[a,b], C. Quaranta[a,b], S. Rahatlou[a,b], C. Rovelli[a], F. Santanastasio[a,b], L. Soffi[a,b]

INFN Sezione di Torino [a], Università di Torino [b], Torino, Italy, Università del Piemonte Orientale [c], Novara, Italy
N. Amapane[a,b], R. Arcidiacono[a,c], S. Argiro[a,b], M. Arneodo[a,c], N. Bartosik[a], R. Bellan[a,b], A. Bellora, C. Biino[a], A. Cappati[a,b], N. Cartiglia[a], S. Cometti[a], M. Costa[a,b], R. Covarelli[a,b], N. Demaria[a], B. Kiani[a,b], C. Mariotti[a], S. Maselli[a], E. Migliore[a,b], V. Monaco[a,b], E. Monteil[a,b], M. Monteno[a], M.M. Obertino[a,b], G. Ortona[a,b], L. Pacher[a,b], N. Pastrone[a], M. Pelliccioni[a], G.L. Pinna Angioni[a,b], A. Romero[a,b], M. Ruspa[a,c], R. Salvatico[a,b], V. Sola[a], A. Solano[a,b], D. Soldi[a,b], A. Staiano[a]

INFN Sezione di Trieste [a], Università di Trieste [b], Trieste, Italy
S. Belforte[a], V. Candelise[a,b], M. Casarsa[a], F. Cossutti[a], A. Da Rold[a,b], G. Della Ricca[a,b], F. Vazzoler[a,b], A. Zanetti[a]

Kyungpook National University, Daegu, Korea
B. Kim, D.H. Kim, G.N. Kim, J. Lee, S.W. Lee, C.S. Moon, Y.D. Oh, S.I. Pak, S. Sekmen, D.C. Son, Y.C. Yang

Chonnam National University, Institute for Universe and Elementary Particles, Kwangju, Korea
H. Kim, D.H. Moon, G. Oh

Hanyang University, Seoul, Korea
B. Francois, T.J. Kim, J. Park

Korea University, Seoul, Korea
S. Cho, S. Choi, Y. Go, D. Gyun, S. Ha, B. Hong, K. Lee, K.S. Lee, J. Lim, J. Park, S.K. Park, Y. Roh, J. Yoo

Kyung Hee University, Department of Physics
J. Goh

Sejong University, Seoul, Korea
H.S. Kim

Seoul National University, Seoul, Korea
J. Almond, J.H. Bhyun, J. Choi, S. Jeon, J. Kim, J.S. Kim, H. Lee, K. Lee, S. Lee, K. Nam, M. Oh, S.B. Oh, B.C. Radburn-Smith, U.K. Yang, H.D. Yoo, I. Yoon, G.B. Yu

University of Seoul, Seoul, Korea
D. Jeon, H. Kim, J.H. Kim, J.S.H. Lee, I.C. Park, I.J Watson

Sungkyunkwan University, Suwon, Korea
Y. Choi, C. Hwang, Y. Jeong, J. Lee, Y. Lee, I. Yu

Riga Technical University, Riga, Latvia
V. Veckalns[32]

Vilnius University, Vilnius, Lithuania
V. Dudenas, A. Juodagalvis, G. Tamulaitis, J. Vaitkus

National Centre for Particle Physics, Universiti Malaya, Kuala Lumpur, Malaysia
Z.A. Ibrahim, F. Mohamad Idris[33], W.A.T. Wan Abdullah, M.N. Yusli, Z. Zolkapli

Universidad de Sonora (UNISON), Hermosillo, Mexico
J.F. Benitez, A. Castaneda Hernandez, J.A. Murillo Quijada, L. Valencia Palomo

Centro de Investigacion y de Estudios Avanzados del IPN, Mexico City, Mexico
H. Castilla-Valdez, E. De La Cruz-Burelo, I. Heredia-De La Cruz[34], R. Lopez-Fernandez, A. Sanchez-Hernandez

Universidad Iberoamericana, Mexico City, Mexico
S. Carrillo Moreno, C. Oropeza Barrera, M. Ramirez-Garcia, F. Vazquez Valencia

Benemerita Universidad Autonoma de Puebla, Puebla, Mexico
J. Eysermans, I. Pedraza, H.A. Salazar Ibarguen, C. Uribe Estrada

Universidad Autónoma de San Luis Potosí, San Luis Potosí, Mexico
A. Morelos Pineda

University of Montenegro, Podgorica, Montenegro
J. Mijuskovic, N. Raicevic

University of Auckland, Auckland, New Zealand
D. Krofcheck

University of Canterbury, Christchurch, New Zealand
S. Bheesette, P.H. Butler

National Centre for Physics, Quaid-I-Azam University, Islamabad, Pakistan
A. Ahmad, M. Ahmad, Q. Hassan, H.R. Hoorani, W.A. Khan, M.A. Shah, M. Shoaib, M. Waqas

AGH University of Science and Technology Faculty of Computer Science, Electronics and Telecommunications, Krakow, Poland
V. Avati, L. Grzanka, M. Malawski

National Centre for Nuclear Research, Swierk, Poland
H. Bialkowska, M. Bluj, B. Boimska, M. Górski, M. Kazana, M. Szleper, P. Zalewski

Institute of Experimental Physics, Faculty of Physics, University of Warsaw, Warsaw, Poland
K. Bunkowski, A. Byszuk[35], K. Doroba, A. Kalinowski, M. Konecki, J. Krolikowski, M. Misiura, M. Olszewski, M. Walczak

Laboratório de Instrumentação e Física Experimental de Partículas, Lisboa, Portugal
M. Araujo, P. Bargassa, D. Bastos, A. Di Francesco, P. Faccioli, B. Galinhas, M. Gallinaro, J. Hollar, N. Leonardo, J. Seixas, K. Shchelina, G. Strong, O. Toldaiev, J. Varela

Joint Institute for Nuclear Research, Dubna, Russia
V. Alexakhin, P. Bunin, I. Golutvin, I. Gorbunov, A. Kamenev, V. Karjavine, V. Korenkov, A. Lanev, A. Malakhov, V. Matveev[36,37], P. Moisenz, V. Palichik, V. Perelygin, M. Savina, S. Shmatov, S. Shulha, V. Trofimov, N. Voytishin, A. Zarubin, V. Zhiltsov

Petersburg Nuclear Physics Institute, Gatchina (St. Petersburg), Russia
L. Chtchipounov, V. Golovtcov, Y. Ivanov, V. Kim[38], E. Kuznetsova[39], P. Levchenko, V. Murzin, V. Oreshkin, I. Smirnov, D. Sosnov, V. Sulimov, L. Uvarov, A. Vorobyev

Institute for Nuclear Research, Moscow, Russia
Yu. Andreev, A. Dermenev, S. Gninenko, N. Golubev, A. Karneyeu, M. Kirsanov, N. Krasnikov, A. Pashenkov, D. Tlisov, A. Toropin

Institute for Theoretical and Experimental Physics named by A.I. Alikhanov of NRC 'Kurchatov Institute', Moscow, Russia
V. Epshteyn, V. Gavrilov, N. Lychkovskaya, A. Nikitenko[40], V. Popov, I. Pozdnyakov, G. Safronov, A. Spiridonov, A. Stepennov, M. Toms, E. Vlasov, A. Zhokin

Moscow Institute of Physics and Technology, Moscow, Russia
T. Aushev

National Research Nuclear University 'Moscow Engineering Physics Institute' (MEPhI), Moscow, Russia
M. Chadeeva[41], P. Parygin, D. Philippov, E. Popova, V. Rusinov

P.N. Lebedev Physical Institute, Moscow, Russia
V. Andreev, M. Azarkin, I. Dremin, M. Kirakosyan, A. Terkulov

Skobeltsyn Institute of Nuclear Physics, Lomonosov Moscow State University, Moscow, Russia
A. Belyaev, E. Boos, V. Bunichev, M. Dubinin[42], L. Dudko, A. Ershov, A. Gribushin, V. Klyukhin, O. Kodolova, I. Lokhtin, S. Obraztsov, V. Savrin, A. Snigirev

Novosibirsk State University (NSU), Novosibirsk, Russia
A. Barnyakov[43], V. Blinov[43], T. Dimova[43], L. Kardapoltsev[43], Y. Skovpen[43]

Institute for High Energy Physics of National Research Centre 'Kurchatov Institute', Protvino, Russia
I. Azhgirey, I. Bayshev, S. Bitioukov, V. Kachanov, D. Konstantinov, P. Mandrik, V. Petrov, R. Ryutin, S. Slabospitskii, A. Sobol, S. Troshin, N. Tyurin, A. Uzunian, A. Volkov

National Research Tomsk Polytechnic University, Tomsk, Russia
A. Babaev, A. Iuzhakov, V. Okhotnikov

Tomsk State University, Tomsk, Russia
V. Borchsh, V. Ivanchenko, E. Tcherniaev

University of Belgrade: Faculty of Physics and VINCA Institute of Nuclear Sciences
P. Adzic[44], P. Cirkovic, D. Devetak, M. Dordevic, P. Milenovic, J. Milosevic, M. Stojanovic

Centro de Investigaciones Energéticas Medioambientales y Tecnológicas (CIEMAT), Madrid, Spain
M. Aguilar-Benitez, J. Alcaraz Maestre, A. lvarez Fernández, I. Bachiller, M. Barrio Luna, J.A. Brochero Cifuentes, C.A. Carrillo Montoya, M. Cepeda, M. Cerrada, N. Colino, B. De La Cruz, A. Delgado Peris, C. Fernandez Bedoya, J.P. Fernández Ramos, J. Flix, M.C. Fouz, O. Gonzalez Lopez, S. Goy Lopez, J.M. Hernandez, M.I. Josa, D. Moran, . Navarro Tobar, A. Pérez-Calero Yzquierdo, J. Puerta Pelayo, I. Redondo, L. Romero, S. Sánchez Navas, M.S. Soares, A. Triossi, C. Willmott

Universidad Autónoma de Madrid, Madrid, Spain
C. Albajar, J.F. de Trocóniz, R. Reyes-Almanza

Universidad de Oviedo, Instituto Universitario de Ciencias y Tecnologías Espaciales de Asturias (ICTEA), Oviedo, Spain
B. Alvarez Gonzalez, J. Cuevas, C. Erice, J. Fernandez Menendez, S. Folgueras, I. Gonzalez Caballero, J.R. González Fernández, E. Palencia Cortezon, V. Rodríguez Bouza, S. Sanchez Cruz

Instituto de Física de Cantabria (IFCA), CSIC-Universidad de Cantabria, Santander, Spain
I.J. Cabrillo, A. Calderon, B. Chazin Quero, J. Duarte Campderros, M. Fernandez, P.J. Fernández Manteca, A. García Alonso, G. Gomez, C. Martinez Rivero, P. Martinez Ruiz del Arbol, F. Matorras, J. Piedra Gomez, C. Prieels, T. Rodrigo, A. Ruiz-Jimeno, L. Russo[45], L. Scodellaro, N. Trevisani, I. Vila, J.M. Vizan Garcia

University of Colombo, Colombo, Sri Lanka
K. Malagalage

University of Ruhuna, Department of Physics, Matara, Sri Lanka
W.G.D. Dharmaratna, N. Wickramage

CERN, European Organization for Nuclear Research, Geneva, Switzerland
D. Abbaneo, B. Akgun, E. Auffray, G. Auzinger, J. Baechler, P. Baillon, A.H. Ball, D. Barney, J. Bendavid, M. Bianco, A. Bocci, P. Bortignon, E. Bossini, C. Botta, E. Brondolin, T. Camporesi, A. Caratelli, G. Cerminara, E. Chapon, G. Cucciati, D. d'Enterria, A. Dabrowski, N. Daci, V. Daponte, A. David, O. Davignon, A. De Roeck, N. Deelen, M. Deile, M. Dobson, M. Dünser, N. Dupont, A. Elliott-Peisert, N. Emriskova, F. Fallavollita[46], D. Fasanella, S. Fiorendi, G. Franzoni, J. Fulcher, W. Funk, S. Giani, D. Gigi, A. Gilbert, K. Gill, F. Glege, M. Gruchala, M. Guilbaud, D. Gulhan, J. Hegeman, C. Heidegger, Y. Iiyama, V. Innocente, P. Janot, O. Karacheban[19], J. Kaspar, J. Kieseler, M. Krammer[1], N. Kratochwil, C. Lange, P. Lecoq, C. Lourenço, L. Malgeri, M. Mannelli, A. Massironi, F. Meijers, J.A. Merlin, S. Mersi, E. Meschi, F. Moortgat, M. Mulders, J. Ngadiuba, J. Niedziela, S. Nourbakhsh, S. Orfanelli, L. Orsini, F. Pantaleo[16], L. Pape, E. Perez, M. Peruzzi, A. Petrilli, G. Petrucciani, A. Pfeiffer, M. Pierini, F.M. Pitters, D. Rabady, A. Racz, M. Rieger, M. Rovere, H. Sakulin, C. Schäfer, C. Schwick, M. Selvaggi, A. Sharma, P. Silva, W. Snoeys, P. Sphicas[47], J. Steggemann, S. Summers, V.R. Tavolaro, D. Treille, A. Tsirou, G.P. Van Onsem, A. Vartak, M. Verzetti, W.D. Zeuner

Paul Scherrer Institut, Villigen, Switzerland
L. Caminada[48], K. Deiters, W. Erdmann, R. Horisberger, Q. Ingram, H.C. Kaestli, D. Kotlinski, U. Langenegger, T. Rohe, S.A. Wiederkehr

ETH Zurich - Institute for Particle Physics and Astrophysics (IPA), Zurich, Switzerland
M. Backhaus, P. Berger, N. Chernyavskaya, G. Dissertori, M. Dittmar, M. Donegà, C. Dorfer, T.A. Gómez Espinosa, C. Grab, D. Hits, T. Klijnsma, W. Lustermann, R.A. Manzoni, M. Marionneau, M.T. Meinhard, F. Micheli, P. Musella, F. Nessi-Tedaldi, F. Pauss, G. Perrin, L. Perrozzi, S. Pigazzini, M.G. Ratti, M. Reichmann, C. Reissel, T. Reitenspiess, D. Ruini, D.A. Sanz Becerra, M. Schönenberger, L. Shchutska, M.L. Vesterbacka Olsson, R. Wallny, D.H. Zhu

Universität Zürich, Zurich, Switzerland
T.K. Aarrestad, C. Amsler[49], D. Brzhechko, M.F. Canelli, A. De Cosa, R. Del Burgo, S. Donato, B. Kilminster, S. Leontsinis, V.M. Mikuni, I. Neutelings, G. Rauco, P. Robmann, D. Salerno, K. Schweiger, C. Seitz, Y. Takahashi, S. Wertz, A. Zucchetta

National Central University, Chung-Li, Taiwan
T.H. Doan, C.M. Kuo, W. Lin, A. Roy, S.S. Yu

National Taiwan University (NTU), Taipei, Taiwan
P. Chang, Y. Chao, K.F. Chen, P.H. Chen, W.-S. Hou, Y.y. Li, R.-S. Lu, E. Paganis, A. Psallidas, A. Steen

Chulalongkorn University, Faculty of Science, Department of Physics, Bangkok, Thailand
B. Asavapibhop, C. Asawatangtrakuldee, N. Srimanobhas, N. Suwonjandee

ukurova University, Physics Department, Science and Art Faculty, Adana, Turkey
A. Bat, F. Boran, A. Celik[50], S. Cerci[51], S. Damarseckin[52], Z.S. Demiroglu, F. Dolek, C. Dozen, I. Dumanoglu, G. Gokbulut, EmineGurpinar Guler[53], Y. Guler, I. Hos[54], C. Isik, E.E. Kangal[55], O. Kara, A. Kayis Topaksu, U. Kiminsu, M. Oglakci, G. Onengut, K. Ozdemir[56], S. Ozturk[57], A.E. Simsek, D. Sunar Cerci[51], U.G. Tok, S. Turkcapar, I.S. Zorbakir, C. Zorbilmez

Middle East Technical University, Physics Department, Ankara, Turkey
B. Isildak[58], G. Karapinar[59], M. Yalvac

Bogazici University, Istanbul, Turkey
I.O. Atakisi, E. Gülmez, M. Kaya[60], O. Kaya[61], Ö. Özçelik, S. Tekten, E.A. Yetkin[62]

Istanbul Technical University, Istanbul, Turkey
A. Cakir, K. Cankocak, Y. Komurcu, S. Sen[63]

Istanbul University, Istanbul, Turkey
B. Kaynak, S. Ozkorucuklu

Institute for Scintillation Materials of National Academy of Science of Ukraine, Kharkov, Ukraine
B. Grynyov

National Scientific Center, Kharkov Institute of Physics and Technology, Kharkov, Ukraine
L. Levchuk

University of Bristol, Bristol, United Kingdom
F. Ball, E. Bhal, S. Bologna, J.J. Brooke, D. Burns[64], E. Clement, D. Cussans, H. Flacher, J. Goldstein, G.P. Heath, H.F. Heath, L. Kreczko, S. Paramesvaran, B. Penning, T. Sakuma, S. Seif El Nasr-Storey, V.J. Smith, J. Taylor, A. Titterton

Rutherford Appleton Laboratory, Didcot, United Kingdom
K.W. Bell, A. Belyaev[65], C. Brew, R.M. Brown, D. Cieri, D.J.A. Cockerill, J.A. Coughlan, K. Harder, S. Harper, J. Linacre, K. Manolopoulos, D.M. Newbold, E. Olaiya, D. Petyt, T. Reis, T. Schuh, C.H. Shepherd-Themistocleous, A. Thea, I.R. Tomalin, T. Williams, W.J. Womersley

Imperial College, London, United Kingdom
R. Bainbridge, P. Bloch, J. Borg, S. Breeze, O. Buchmuller, A. Bundock, GurpreetSingh CHAHAL[66], D. Colling, P. Dauncey, G. Davies, M. Della Negra, R. Di Maria, P. Everaerts, G. Hall, G. Iles, T. James, M. Komm, C. Laner, L. Lyons, A.-M. Magnan, S. Malik, A. Martelli, V. Milosevic, J. Nash[67], V. Palladino, M. Pesaresi, D.M. Raymond, A. Richards, A. Rose, E. Scott, C. Seez, A. Shtipliyski, M. Stoye, T. Strebler, A. Tapper, K. Uchida, T. Virdee[16], N. Wardle, D. Winterbottom, J. Wright, A.G. Zecchinelli, S.C. Zenz

Brunel University, Uxbridge, United Kingdom
J.E. Cole, P.R. Hobson, A. Khan, P. Kyberd, C.K. Mackay, A. Morton, I.D. Reid, L. Teodorescu, S. Zahid

Baylor University, Waco, USA
K. Call, B. Caraway, J. Dittmann, K. Hatakeyama, C. Madrid, B. McMaster, N. Pastika, C. Smith

Catholic University of America, Washington, DC, USA
R. Bartek, A. Dominguez, R. Uniyal, A.M. Vargas Hernandez

The University of Alabama, Tuscaloosa, USA
A. Buccilli, S.I. Cooper, C. Henderson, P. Rumerio, C. West

Boston University, Boston, USA
D. Arcaro, Z. Demiragli, D. Gastler, D. Pinna, C. Richardson, J. Rohlf, D. Sperka, I. Suarez, L. Sulak, D. Zou

Brown University, Providence, USA
G. Benelli, B. Burkle, X. Coubez[17], D. Cutts, Y.t. Duh, M. Hadley, J. Hakala, U. Heintz, J.M. Hogan[68], K.H.M. Kwok, E. Laird, G. Landsberg, J. Lee, Z. Mao, M. Narain, S. Sagir[69], R. Syarif, E. Usai, D. Yu, W. Zhang

University of California, Davis, Davis, USA
R. Band, C. Brainerd, R. Breedon, M. Calderon De La Barca Sanchez, M. Chertok, J. Conway, R. Conway, P.T. Cox, R. Erbacher, C. Flores, G. Funk, F. Jensen, W. Ko, O. Kukral, R. Lander, M. Mulhearn, D. Pellett, J. Pilot, M. Shi, D. Taylor, K. Tos, M. Tripathi, Z. Wang, F. Zhang

University of California, Los Angeles, USA
M. Bachtis, C. Bravo, R. Cousins, A. Dasgupta, A. Florent, J. Hauser, M. Ignatenko, N. Mccoll, W.A. Nash, S. Regnard, D. Saltzberg, C. Schnaible, B. Stone, V. Valuev

University of California, Riverside, Riverside, USA
K. Burt, Y. Chen, R. Clare, J.W. Gary, S.M.A. Ghiasi Shirazi, G. Hanson, G. Karapostoli, E. Kennedy, O.R. Long, M. Olmedo Negrete, M.I. Paneva, W. Si, L. Wang, S. Wimpenny, B.R. Yates, Y. Zhang

University of California, San Diego, La Jolla, USA
J.G. Branson, P. Chang, S. Cittolin, M. Derdzinski, R. Gerosa, D. Gilbert, B. Hashemi, D. Klein, V. Krutelyov, J. Letts, M. Masciovecchio, S. May, S. Padhi, M. Pieri, V. Sharma, M. Tadel, F. Würthwein, A. Yagil, G. Zevi Della Porta

University of California, Santa Barbara - Department of Physics, Santa Barbara, USA
N. Amin, R. Bhandari, C. Campagnari, M. Citron, V. Dutta, M. Franco Sevilla, L. Gouskos, J. Incandela, B. Marsh, H. Mei, A. Ovcharova, H. Qu, J. Richman, U. Sarica, D. Stuart, S. Wang

California Institute of Technology, Pasadena, USA
D. Anderson, A. Bornheim, O. Cerri, I. Dutta, J.M. Lawhorn, N. Lu, J. Mao, H.B. Newman, T.Q. Nguyen, J. Pata, M. Spiropulu, J.R. Vlimant, S. Xie, Z. Zhang, R.Y. Zhu

Carnegie Mellon University, Pittsburgh, USA
M.B. Andrews, T. Ferguson, T. Mudholkar, M. Paulini, M. Sun, I. Vorobiev, M. Weinberg

University of Colorado Boulder, Boulder, USA
J.P. Cumalat, W.T. Ford, A. Johnson, E. MacDonald, T. Mulholland, R. Patel, A. Perloff, K. Stenson, K.A. Ulmer, S.R. Wagner

Cornell University, Ithaca, USA
J. Alexander, J. Chaves, Y. Cheng, J. Chu, A. Datta, A. Frankenthal, K. Mcdermott, J.R. Patterson, D. Quach, A. Rinkevicius[70], A. Ryd, S.M. Tan, Z. Tao, J. Thom, P. Wittich, M. Zientek

Fermi National Accelerator Laboratory, Batavia, USA
S. Abdullin, M. Albrow, M. Alyari, G. Apollinari, A. Apresyan, A. Apyan, S. Banerjee, L.A.T. Bauerdick, A. Beretvas, J. Berryhill, P.C. Bhat, K. Burkett, J.N. Butler, A. Canepa,

G.B. Cerati, H.W.K. Cheung, F. Chlebana, M. Cremonesi, J. Duarte, V.D. Elvira, J. Freeman, Z. Gecse, E. Gottschalk, L. Gray, D. Green, S. Grünendahl, O. Gutsche, AllisonReinsvold Hall, J. Hanlon, R.M. Harris, S. Hasegawa, R. Heller, J. Hirschauer, B. Jayatilaka, S. Jindariani, M. Johnson, U. Joshi, B. Klima, M.J. Kortelainen, B. Kreis, S. Lammel, J. Lewis, D. Lincoln, R. Lipton, M. Liu, T. Liu, J. Lykken, K. Maeshima, J.M. Marraffino, D. Mason, P. McBride, P. Merkel, S. Mrenna, S. Nahn, V. O'Dell, V. Papadimitriou, K. Pedro, C. Pena, G. Rakness, F. Ravera, L. Ristori, B. Schneider, E. Sexton-Kennedy, N. Smith, A. Soha, W.J. Spalding, L. Spiegel, S. Stoynev, J. Strait, N. Strobbe, L. Taylor, S. Tkaczyk, N.V. Tran, L. Uplegger, E.W. Vaandering, C. Vernieri, R. Vidal, M. Wang, H.A. Weber

University of Florida, Gainesville, USA
D. Acosta, P. Avery, D. Bourilkov, A. Brinkerhoff, L. Cadamuro, A. Carnes, V. Cherepanov, D. Curry, F. Errico, R.D. Field, S.V. Gleyzer, B.M. Joshi, M. Kim, J. Konigsberg, A. Korytov, K.H. Lo, P. Ma, K. Matchev, N. Menendez, G. Mitselmakher, D. Rosenzweig, K. Shi, J. Wang, S. Wang, X. Zuo

Florida International University, Miami, USA
Y.R. Joshi

Florida State University, Tallahassee, USA
T. Adams, A. Askew, S. Hagopian, V. Hagopian, K.F. Johnson, R. Khurana, T. Kolberg, G. Martinez, T. Perry, H. Prosper, C. Schiber, R. Yohay, J. Zhang

Florida Institute of Technology, Melbourne, USA
M.M. Baarmand, M. Hohlmann, D. Noonan, M. Rahmani, M. Saunders, F. Yumiceva

University of Illinois at Chicago (UIC), Chicago, USA
M.R. Adams, L. Apanasevich, D. Berry, R.R. Betts, R. Cavanaugh, X. Chen, S. Dittmer, O. Evdokimov, C.E. Gerber, D.A. Hangal, D.J. Hofman, K. Jung, C. Mills, T. Roy, M.B. Tonjes, N. Varelas, J. Viinikainen, H. Wang, X. Wang, Z. Wu

The University of Iowa, Iowa City, USA
M. Alhusseini, B. Bilki[53], W. Clarida, K. Dilsiz[71], S. Durgut, R.P. Gandrajula, M. Haytmyradov, V. Khristenko, O.K. Köseyan, J.-P. Merlo, A. Mestvirishvili[72], A. Moeller, J. Nachtman, H. Ogul[73], Y. Onel, F. Ozok[74], A. Penzo, C. Snyder, E. Tiras, J. Wetzel

Johns Hopkins University, Baltimore, USA
B. Blumenfeld, A. Cocoros, N. Eminizer, D. Fehling, L. Feng, A.V. Gritsan, W.T. Hung, P. Maksimovic, J. Roskes, M. Swartz

The University of Kansas, Lawrence, USA
C. Baldenegro Barrera, P. Baringer, A. Bean, S. Boren, J. Bowen, A. Bylinkin, T. Isidori, S. Khalil, J. King, G. Krintiras, A. Kropivnitskaya, C. Lindsey, D. Majumder, W. Mcbrayer, N. Minafra, M. Murray, C. Rogan, C. Royon, S. Sanders, E. Schmitz, J.D. Tapia Takaki, Q. Wang, J. Williams, G. Wilson

Kansas State University, Manhattan, USA
S. Duric, A. Ivanov, K. Kaadze, D. Kim, Y. Maravin, D.R. Mendis, T. Mitchell, A. Modak, A. Mohammadi

Lawrence Livermore National Laboratory, Livermore, USA
F. Rebassoo, D. Wright

University of Maryland, College Park, USA
A. Baden, O. Baron, A. Belloni, S.C. Eno, Y. Feng, N.J. Hadley, S. Jabeen, G.Y. Jeng, R.G. Kellogg,

J. Kunkle, A.C. Mignerey, S. Nabili, F. Ricci-Tam, M. Seidel, Y.H. Shin, A. Skuja, S.C. Tonwar, K. Wong

Massachusetts Institute of Technology, Cambridge, USA
D. Abercrombie, B. Allen, A. Baty, R. Bi, S. Brandt, W. Busza, I.A. Cali, M. D'Alfonso, G. Gomez Ceballos, M. Goncharov, P. Harris, D. Hsu, M. Hu, M. Klute, D. Kovalskyi, Y.-J. Lee, P.D. Luckey, B. Maier, A.C. Marini, C. Mcginn, C. Mironov, S. Narayanan, X. Niu, C. Paus, D. Rankin, C. Roland, G. Roland, Z. Shi, G.S.F. Stephans, K. Sumorok, K. Tatar, D. Velicanu, J. Wang, T.W. Wang, B. Wyslouch

University of Minnesota, Minneapolis, USA
A.C. Benvenuti[†], R.M. Chatterjee, A. Evans, S. Guts, P. Hansen, J. Hiltbrand, Y. Kubota, Z. Lesko, J. Mans, R. Rusack, M.A. Wadud

University of Mississippi, Oxford, USA
J.G. Acosta, S. Oliveros

University of Nebraska-Lincoln, Lincoln, USA
K. Bloom, D.R. Claes, C. Fangmeier, L. Finco, F. Golf, R. Gonzalez Suarez, R. Kamalieddin, I. Kravchenko, J.E. Siado, G.R. Snow[†], B. Stieger, W. Tabb

State University of New York at Buffalo, Buffalo, USA
G. Agarwal, C. Harrington, I. Iashvili, A. Kharchilava, C. McLean, D. Nguyen, A. Parker, J. Pekkanen, S. Rappoccio, B. Roozbahani

Northeastern University, Boston, USA
G. Alverson, E. Barberis, C. Freer, Y. Haddad, A. Hortiangtham, G. Madigan, D.M. Morse, T. Orimoto, L. Skinnari, A. Tishelman-Charny, T. Wamorkar, B. Wang, A. Wisecarver, D. Wood

Northwestern University, Evanston, USA
S. Bhattacharya, J. Bueghly, T. Gunter, K.A. Hahn, N. Odell, M.H. Schmitt, K. Sung, M. Trovato, M. Velasco

University of Notre Dame, Notre Dame, USA
R. Bucci, N. Dev, R. Goldouzian, M. Hildreth, K. Hurtado Anampa, C. Jessop, D.J. Karmgard, K. Lannon, W. Li, N. Loukas, N. Marinelli, I. Mcalister, F. Meng, C. Mueller, Y. Musienko[36], M. Planer, R. Ruchti, P. Siddireddy, G. Smith, S. Taroni, M. Wayne, A. Wightman, M. Wolf, A. Woodard

The Ohio State University, Columbus, USA
J. Alimena, B. Bylsma, L.S. Durkin, S. Flowers, B. Francis, C. Hill, W. Ji, A. Lefeld, T.Y. Ling, B.L. Winer

Princeton University, Princeton, USA
S. Cooperstein, G. Dezoort, P. Elmer, J. Hardenbrook, N. Haubrich, S. Higginbotham, A. Kalogeropoulos, S. Kwan, D. Lange, M.T. Lucchini, J. Luo, D. Marlow, K. Mei, I. Ojalvo, J. Olsen, C. Palmer, P. Piroué, J. Salfeld-Nebgen, D. Stickland, C. Tully, Z. Wang

University of Puerto Rico, Mayaguez, USA
S. Malik, S. Norberg

Purdue University, West Lafayette, USA
A. Barker, V.E. Barnes, S. Das, L. Gutay, M. Jones, A.W. Jung, A. Khatiwada, B. Mahakud, D.H. Miller, G. Negro, N. Neumeister, C.C. Peng, S. Piperov, H. Qiu, J.F. Schulte, J. Sun, F. Wang, R. Xiao, W. Xie

Purdue University Northwest, Hammond, USA
T. Cheng, J. Dolen, N. Parashar

Rice University, Houston, USA
U. Behrens, K.M. Ecklund, S. Freed, F.J.M. Geurts, M. Kilpatrick, Arun Kumar, W. Li, B.P. Padley, R. Redjimi, J. Roberts, J. Rorie, W. Shi, A.G. Stahl Leiton, Z. Tu, A. Zhang

University of Rochester, Rochester, USA
A. Bodek, P. de Barbaro, R. Demina, J.L. Dulemba, C. Fallon, T. Ferbel, M. Galanti, A. Garcia-Bellido, O. Hindrichs, A. Khukhunaishvili, E. Ranken, P. Tan, R. Taus

Rutgers, The State University of New Jersey, Piscataway, USA
B. Chiarito, J.P. Chou, A. Gandrakota, Y. Gershtein, E. Halkiadakis, A. Hart, M. Heindl, E. Hughes, S. Kaplan, S. Kyriacou, I. Laflotte, A. Lath, R. Montalvo, K. Nash, M. Osherson, H. Saka, S. Salur, S. Schnetzer, S. Somalwar, R. Stone, S. Thomas

University of Tennessee, Knoxville, USA
H. Acharya, A.G. Delannoy, G. Riley, S. Spanier

Texas A&M University, College Station, USA
O. Bouhali[75], M. Dalchenko, M. De Mattia, A. Delgado, S. Dildick, R. Eusebi, J. Gilmore, T. Huang, T. Kamon[76], S. Luo, D. Marley, R. Mueller, D. Overton, L. Perniè, D. Rathjens, A. Safonov

Texas Tech University, Lubbock, USA
N. Akchurin, J. Damgov, F. De Guio, S. Kunori, K. Lamichhane, S.W. Lee, T. Mengke, S. Muthumuni, T. Peltola, S. Undleeb, I. Volobouev, Z. Wang, A. Whitbeck

Vanderbilt University, Nashville, USA
S. Greene, A. Gurrola, R. Janjam, W. Johns, C. Maguire, A. Melo, H. Ni, K. Padeken, F. Romeo, P. Sheldon, S. Tuo, J. Velkovska, M. Verweij

University of Virginia, Charlottesville, USA
M.W. Arenton, P. Barria, B. Cox, G. Cummings, R. Hirosky, M. Joyce, A. Ledovskoy, C. Neu, B. Tannenwald, Y. Wang, E. Wolfe, F. Xia

Wayne State University, Detroit, USA
R. Harr, P.E. Karchin, N. Poudyal, J. Sturdy, P. Thapa

University of Wisconsin - Madison, Madison, WI, USA
T. Bose, J. Buchanan, C. Caillol, D. Carlsmith, S. Dasu, I. De Bruyn, L. Dodd, F. Fiori, C. Galloni, B. Gomber[77], H. He, M. Herndon, A. Hervé, U. Hussain, P. Klabbers, A. Lanaro, A. Loeliger, K. Long, R. Loveless, J. Madhusudanan Sreekala, T. Ruggles, A. Savin, V. Sharma, W.H. Smith, D. Teague, S. Trembath-reichert, N. Woods

†: Deceased
1: Also at Vienna University of Technology, Vienna, Austria
2: Also at IRFU, CEA, Université Paris-Saclay, Gif-sur-Yvette, France
3: Also at Universidade Estadual de Campinas, Campinas, Brazil
4: Also at Federal University of Rio Grande do Sul, Porto Alegre, Brazil
5: Also at UFMS, Nova Andradina, Brazil
6: Also at Universidade Federal de Pelotas, Pelotas, Brazil
7: Also at Université Libre de Bruxelles, Bruxelles, Belgium
8: Also at University of Chinese Academy of Sciences, Beijing, China
9: Also at Institute for Theoretical and Experimental Physics named by A.I. Alikhanov of NRC

'Kurchatov Institute', Moscow, Russia
10: Also at Joint Institute for Nuclear Research, Dubna, Russia
11: Also at Ain Shams University, Cairo, Egypt
12: Also at Zewail City of Science and Technology, Zewail, Egypt
13: Also at Purdue University, West Lafayette, USA
14: Also at Université de Haute Alsace, Mulhouse, France
15: Also at Erzincan Binali Yildirim University, Erzincan, Turkey
16: Also at CERN, European Organization for Nuclear Research, Geneva, Switzerland
17: Also at RWTH Aachen University, III. Physikalisches Institut A, Aachen, Germany
18: Also at University of Hamburg, Hamburg, Germany
19: Also at Brandenburg University of Technology, Cottbus, Germany
20: Also at Institute of Physics, University of Debrecen, Debrecen, Hungary, Debrecen, Hungary
21: Also at Institute of Nuclear Research ATOMKI, Debrecen, Hungary
22: Also at MTA-ELTE Lendület CMS Particle and Nuclear Physics Group, Eötvös Loránd University, Budapest, Hungary, Budapest, Hungary
23: Also at IIT Bhubaneswar, Bhubaneswar, India, Bhubaneswar, India
24: Also at Institute of Physics, Bhubaneswar, India
25: Also at Shoolini University, Solan, India
26: Also at University of Visva-Bharati, Santiniketan, India
27: Also at Isfahan University of Technology, Isfahan, Iran
28: Now at INFN Sezione di Bari [a], Università di Bari [b], Politecnico di Bari [c], Bari, Italy
29: Also at Italian National Agency for New Technologies, Energy and Sustainable Economic Development, Bologna, Italy
30: Also at Centro Siciliano di Fisica Nucleare e di Struttura Della Materia, Catania, Italy
31: Also at Scuola Normale e Sezione dell'INFN, Pisa, Italy
32: Also at Riga Technical University, Riga, Latvia, Riga, Latvia
33: Also at Malaysian Nuclear Agency, MOSTI, Kajang, Malaysia
34: Also at Consejo Nacional de Ciencia y Tecnología, Mexico City, Mexico
35: Also at Warsaw University of Technology, Institute of Electronic Systems, Warsaw, Poland
36: Also at Institute for Nuclear Research, Moscow, Russia
37: Now at National Research Nuclear University 'Moscow Engineering Physics Institute' (MEPhI), Moscow, Russia
38: Also at St. Petersburg State Polytechnical University, St. Petersburg, Russia
39: Also at University of Florida, Gainesville, USA
40: Also at Imperial College, London, United Kingdom
41: Also at P.N. Lebedev Physical Institute, Moscow, Russia
42: Also at California Institute of Technology, Pasadena, USA
43: Also at Budker Institute of Nuclear Physics, Novosibirsk, Russia
44: Also at Faculty of Physics, University of Belgrade, Belgrade, Serbia
45: Also at Università degli Studi di Siena, Siena, Italy
46: Also at INFN Sezione di Pavia [a], Università di Pavia [b], Pavia, Italy, Pavia, Italy
47: Also at National and Kapodistrian University of Athens, Athens, Greece
48: Also at Universität Zürich, Zurich, Switzerland
49: Also at Stefan Meyer Institute for Subatomic Physics, Vienna, Austria, Vienna, Austria
50: Also at Burdur Mehmet Akif Ersoy University, BURDUR, Turkey
51: Also at Adiyaman University, Adiyaman, Turkey
52: Also at Şırnak University, Sirnak, Turkey
53: Also at Beykent University, Istanbul, Turkey, Istanbul, Turkey

54: Also at Istanbul Aydin University, Istanbul, Turkey
55: Also at Mersin University, Mersin, Turkey
56: Also at Piri Reis University, Istanbul, Turkey
57: Also at Gaziosmanpasa University, Tokat, Turkey
58: Also at Ozyegin University, Istanbul, Turkey
59: Also at Izmir Institute of Technology, Izmir, Turkey
60: Also at Marmara University, Istanbul, Turkey
61: Also at Kafkas University, Kars, Turkey
62: Also at Istanbul Bilgi University, Istanbul, Turkey
63: Also at Hacettepe University, Ankara, Turkey
64: Also at Vrije Universiteit Brussel, Brussel, Belgium
65: Also at School of Physics and Astronomy, University of Southampton, Southampton, United Kingdom
66: Also at IPPP Durham University, Durham, United Kingdom
67: Also at Monash University, Faculty of Science, Clayton, Australia
68: Also at Bethel University, St. Paul, Minneapolis, USA, St. Paul, USA
69: Also at Karamanoğlu Mehmetbey University, Karaman, Turkey
70: Also at Vilnius University, Vilnius, Lithuania
71: Also at Bingol University, Bingol, Turkey
72: Also at Georgian Technical University, Tbilisi, Georgia
73: Also at Sinop University, Sinop, Turkey
74: Also at Mimar Sinan University, Istanbul, Istanbul, Turkey
75: Also at Texas A&M University at Qatar, Doha, Qatar
76: Also at Kyungpook National University, Daegu, Korea, Daegu, Korea
77: Also at University of Hyderabad, Hyderabad, India